

PATRICIA RICARDINO DA SILVEIRA

**ALTERAÇÕES OXIDATIVAS, MOLECULARES E FISIOLÓGICAS EM
PLANTAS DE MILHO INFECTADAS POR *Exserohilum turcicum***

Tese apresentada à Universidade Federal de Viçosa, como parte das exigências do Programa de Pós-Graduação em Fitopatologia, para obtenção do título de *Doctor Scientiae*.

VIÇOSA
MINAS GERAIS – BRASIL
2016

**Ficha catalográfica preparada pela Biblioteca Central da Universidade
Federal de Viçosa - Câmpus Viçosa**

T

S587a
2016
Silveira, Patricia Ricardino da, 1986-
Alterações oxidativas, moleculares e fisiológicas em plantas
de milho infectadas por *Exserohilum turcicum* / Patricia
Ricardino da Silveira. – Viçosa, MG, 2016.
ix, 69f. : il. (algumas color.) ; 29 cm.

Orientador: Fabrício de Ávila Rodrigues.
Tese (doutorado) - Universidade Federal de Viçosa.
Inclui bibliografia.

1. Milho - Doenças e pragas. 2. *Exserohilum turcicum*.
3. Milho - Fisiologia. 4. Milho - Enzimas. I. Universidade
Federal de Viçosa. Departamento de Fitopatologia. Programa de
Pós-graduação em Fitopatologia. II. Título.

CDD 22 ed. 633.153

PATRICIA RICARDINO DA SILVEIRA

**ALTERAÇÕES OXIDATIVAS, MOLECULARES E FISIOLÓGICAS EM
PLANTAS DE MILHO INFECTADAS POR *Exserohilum turcicum***

Tese apresentada à Universidade Federal de Viçosa, como parte das exigências do Programa de Pós-Graduação em Fitopatologia, para obtenção do título de *Doctor Scientiae*.

APROVADA: 26 de agosto de 2016.

Robert Weingart Barreto

Claudine Márcia de Carvalho

Paulo Cezar Cavatte

Renata Sousa Resende

Fabício de Ávila Rodrigues

(Orientador)

*Aos meus pais, Enir Aparecida Ricardino Silveira
e Delson Ribeiro da Siveira e a minha irmã,
Daniela Ricardino da Silveira.*

AGRADECIMENTOS

A Deus, dono de toda ciência, sabedoria e poder e a Nossa Senhora pelo cuidado.

Aos meus pais, pelo imenso apoio e amor incondicional em todas as horas. À minha querida irmã e aos meus avós queridos.

Ao professor Fabrício de Ávila Rodrigues pela orientação, confiança e paciência.

À Universidade Federal de Viçosa e ao Departamento de Fitopatologia pela oportunidade de realização deste trabalho.

À Coordenação de Aperfeiçoamento de Pessoal de Nível Superior (CAPES) e ao Conselho Nacional de Desenvolvimento Científico e Tecnológico (CNPq) pela concessão da bolsa de estudo.

Aos amigos do laboratório, Carlos, Carla, Renata, Jonas, Isaías, Daniel, Caroline, Maria Izabel, Tássia, Paloma e Emerson pela amizade, boa vontade e disponibilidade em ajudar sempre que precisei.

Aos funcionários do Departamento de Fitopatologia, principalmente ao Bruno, Suely, Daniel, Camilo e Delfin pela imensa força e compreensão.

BIOGRAFIA

Patrícia Ricardino da Silveira, filha de Delson Ribeiro da Silveira e Enir Aparecida Ricardino Silveira, nasceu em 10 de janeiro de 1986 em Lavras - MG.

Iniciou o curso de Agronomia na Universidade Federal de Viçosa, Viçosa, Minas Gerais, Brasil, em março de 2005, recebendo o título de Bacharel Agronomia em janeiro de 2010, pela mesma instituição.

Em agosto de 2010, iniciou o curso de Mestrado no Programa de Pós-Graduação em Fitopatologia na Universidade Federal de Viçosa, submetendo-se à defesa de dissertação em 24 de julho de 2012.

Neste mesmo ano iniciou o curso de Doutorado no Programa de Pós-Graduação em Fitopatologia na Universidade Federal de Viçosa, submetendo-se à defesa da tese em agosto de 2016.

SUMÁRIO

RESUMO	vi
ABSTRACT	viii
GENERAL INTRODUCTION	1
CHAPTER 1	5
The Role of the Antioxidant Metabolism on Maize Leaves During the Infection Process of <i>Exserohilum turcicum</i>	5
Abstract	6
Introduction	7
Materials and Methods	9
Results	17
Discussion	20
References	25
List of Tables and Figures	31
CHAPTER 2	40
Gas Exchange and Chlorophyll <i>a</i> Fluorescence on Maize Leaves Infected by <i>Exserohilum turcicum</i>	40
Abstract	41
Introduction	42
Materials and Methods	44
Results	48
Discussion	51
References	56
List of Tables and Figures	61

RESUMO

SILVEIRA, Patricia Ricardino da, D. Sc., Universidade Federal de Viçosa, agosto de 2016. **Alterações oxidativas, moleculares e fisiológicas em plantas de milho infectadas por *Exserohilum turcicum***. Orientador: Fabrício de Ávila Rodrigues. Coorientador: Gleiber Quintão Furtado.

A queima foliar, causada por *Exserohilum turcicum* é uma doença de grande importância em áreas produtoras de milho em todo o mundo e é responsável por significativas perdas durante a ocorrência de epidemias da doença. O primeiro estudo teve o objetivo de verificar as atividades de enzimas e as expressões dos genes envolvidos metabolismo antioxidativo assim como as concentrações de peróxido de hidrogênio (H_2O_2) e de aldeído malônico (MDA) e a perda de eletrólitos (EL) em plantas de milho infectadas e não infectadas com *E. turcicum*. As atividades das enzimas superóxido dismutase (SOD), catalase (CAT), ascorbato peroxidase (APX), peroxidase (POX), glutaciona redutase (GR), glutaciona-S-transferase (GST) e glutaciona peroxidase (GPX) aumentaram nas plantas infectadas em relação às plantas não infectadas principalmente a partir dos 10 dias após inoculação (dai). A expressão relativa dos genes superóxido dismutase (*sod*), catalase (*cat*), ascorbato peroxidase (*apx*), peroxidase (*pox*), glutaciona redutase (*gr*) and glutaciona-S-transferase (*gst*) foram maiores para as plantas infectadas em comparação com as plantas não infectadas principalmente nos estágios mais avançados da infecção fúngica. As concentrações de H_2O_2 e MDA aumentaram aos 15 e 20 dai para as plantas infectadas em comparação com as não infectadas e a EL aumentou nas plantas infectadas partir dos 10 dai. De uma maneira geral, ocorreu aumento em todas as variáveis estudadas nas plantas infectadas principalmente nas fases finais do processo infeccioso. Em conclusão, uma participação tardia do metabolismo antioxidante nas folhas infectadas não foi útil para minimizar os efeitos deletérios da infecção por *E. turcicum* sua fase necrotrófica. O segundo estudo foi realizado com o objetivo de investigar as alterações fotossintéticas em plantas de milho infectadas por *E. turcicum*. Foram avaliados os parâmetros relacionados às trocas gasosas tais como a taxa de assimilação de carbono (A), a condutância estomática (g_s), a transpiração (E) e a concentração interna de CO_2 (C_i) e os parâmetros da fluorescência da clorofila (Chl) a saber: rendimento quântico máximo do fotossistema II (PSII) (F_v/F_m), rendimento quântico efetivo do PSII ($(Y(II))$), rendimento quântico de

dissipação de energia regulada ($Y(NPQ)$), rendimento quântico de dissipação de energia não regulada ($Y(NO)$) e a taxa de transporte de elétrons (ETR). Além disso, foram determinadas as concentrações dos pigmentos fotossintéticos Chl_a , Chl_b e carotenoides. Os valores de A , g_s , E e C_i diminuíram à medida que os sintomas da doença se desenvolveram. Mudanças nos parâmetros da fluorescência da $Chl a$ tornaram-se evidentes aos 10 dai e mudanças nas imagens começaram a partir dos 5 dai e intensificaram-se em estágios avançados da infecção fúngica. As concentrações de $Chla$, $Chlb$ e carotenoides diminuíram nas folhas das plantas infectadas aos 15 e 20 dai. Os resultados do presente estudo permitiram concluir que a fotossíntese nas folhas das plantas de milho foi dramaticamente afetada durante o processo de infecção de *E. turcicum* principalmente através de limitações de natureza bioquímica e difusiva.

ABSTRACT

SILVEIRA, Patricia Ricardino da, D. Sc., Universidade Federal de Viçosa, august, 2016. **Oxidative, molecular and physiological changes on maize plants infected by *Exserohilum turcicum*.** Adviser: Fabrício de Ávila Rodrigues. Co-adviser: Gleiber Quintão Furtado.

Northern leaf blight (NLB), caused by the fungus *Exserohilum turcicum* is a disease of great importance in producing maize areas worldwide and is responsible for significant losses during the occurrence of disease epidemics. The first study aimed to verify the activities of enzymes and genes expression involved in the antioxidative metabolism as well as the concentration of hydrogen peroxide (H_2O_2) and malondialdehyde (MDA) as well as the electrolyte leakage (EL) in maize plants infected and non-infected with *E. turcicum*. The activities of superoxide dismutase (SOD), catalase (CAT), ascorbate peroxidase (APX), peroxidase (POX), glutathione reductase (GR), glutathione-S-transferase (GST) and glutathione peroxidase (GPX) increased in infected plants compared to non-infected plants mainly from 10 days after inoculation (dai). The relative expression of the genes coding for superoxide dismutase (*sod*), catalase (*cat*), ascorbate peroxidase (*apx*), peroxidase (*pox*), glutathione reductase (*gr*) and glutathione-S-transferase (*gst*) were higher for the infected plants in comparison to the non-infected ones especially at more advanced stages of fungal infection. The H_2O_2 and MDA concentrations increased from 15 and 20 dai for the infected plants in comparison to the non-infected ones and the EL increased for the infected plants from 10 dai. In general, there was an increase in the values for all variables obtained from the infected plants mainly at the final stage of fungal which was accompanied by an increase on disease development. In conclusion, a late involvement of the antioxidant metabolism in the infected leaves was not helpful to counteract the deleterious effects of *E. turcicum* infection at its necrotrophic phase. The second study was carried out to investigate the photosynthetic changes in maize plants infected with *E. turcicum*. The parameters of leaf gas exchange (net carbon assimilation rate ((*A*), stomatal conductance (g_s), transpiration rate (*E*) and internal CO_2 concentration (C_i)) and chlorophyll (Chl) *a* fluorescence (maximum quantum yield of photosystem II (PSII) (F_v/F_m), effective quantum yield of photosystem II (PSII) ((*Y*(II)), quantum yield of regulated energy dissipation ((*Y*(NPQ)), quantum yield of non-regulated energy dissipation ((*Y*(NO)) and electron transport rate (ETR)) were evaluated as well as the concentrations of

photosynthetic pigments Chl_a , Chl_b and carotenoids. The values of A , g_s , E and C_i decreased as the symptoms of NLB developed. Changes in $\text{Chl } a$ fluorescence parameters became evident at 10 days after inoculation (dai) and changes in the images began from 5 dai and intensified at advanced stages of fungal infection. The concentrations of Chl_a , Chl_b and carotenoids decreased in the leaves of infected plants at 15 and 20 dai. In conclusion, the results from the present study demonstrate, for the first time, that the photosynthesis on the leaves of maize plants was dramatically affected during the infection of process of *E. turcicum* mainly through limitations of diffusive and biochemical nature.

GENERAL INTRODUCTION

Northern leaf blight (NLB), caused by the fungus *Exserohilum turcicum* (Pass.) Leonard and Suggs (anamorph) and *Setosphaeria turcica* (Luterell) Leonard and Suggs (teleomorph) (Leonard and Suggs, 1974; Luttrell and Bacon, 1977; Sivanesan, 1984), is a widespread disease in all producing maize areas worldwide and is capable to cause of significant yield losses under conditions favorable for disease such as temperature between 18 and 27°C and high humidity (above 90%) (Adipala et al., 1993; CIMMYT, 2014). The NLB symptoms start in the older leaves as elliptical lesions with necrotic center and chlorotic halos (Munkvold and White, 2016). Plants when exposed to biotic stress conditions such as the attack by pathogens are able to respond by producing reactive oxygen species (ROS) mainly hydrogen peroxide (H₂O₂), superoxide anion radical (O₂⁻) and hydroxyl free radical (OH⁻) (Medhy, 1994). However, excessive ROS can trigger the host cell damage that can lead to events such as lipid peroxidation of cell membranes and oxidation of proteins leading to cell death (Lamb and Dixon, 1997; Arora et al., 2002; Mittler, 2002). In order to mitigate the damage caused by the excess of ROS, plants have developed mechanisms for removal of ROS by producing an enzymatic antioxidant system involving enzymes such as superoxide dismutase (SOD), catalase (CAT), peroxidase (POX), ascorbate peroxidase (APX), glutathione reductase (GR), glutathione-S-transferase (GST) and glutathione peroxidase (GPX) (Mittler, 2002). SOD is the first to act by promoting anion dismutation of O₂⁻ to H₂O₂, which is further detoxified by CAT, POX, APX, GPX and GR (Mittler 2002; Apel and Hirt, 2004). High H₂O₂ concentration also were associated with strong expression of the genes *cat 1*, *cat 2* and *gst* in maize plants showing, therefore, a role of H₂O₂ in the regulation of the antioxidant genes (Polidoros and Scandalios, 1999). Besides the biochemical stress, several studies have shown physiological disorders caused by

various pathogens primarily resulting in significant changes in gas exchange and chlorophyll (Chl) *a* fluorescence of infected plants (Shtienberg, 1992; Jesus Junior et al., 2001; Iqbal et al., 2012). The image analysis of Chl *a* fluorescence has also been used in studies showing physiological changes in plants exposed to environmental stress conditions. It is a non-destructive technique, sensitive and capable of providing a pre-symptomatic diagnosis showing changes in the photosynthetic apparatus of plants infected by pathogens (Rolfe and Scholes, 2010; Gorbe and Calatayud, 2012). The present study aimed to investigate the changes in the antioxidant metabolism of maize leaves during the infection process of *E. turcicum* by examining the production of ROS as well as the expression of genes and the activities of the major enzymes involved in this process as well as photosynthetic performance through analysis of gas exchange parameters associated with fluorescence imaging technique of Chl *a* and the concentration of photosynthetic pigments.

References

- Adipala E, Lipps PE, Madden LV, 1993. Reaction of maize cultivars from Uganda to *Exserohilum turcicum*. *Phytopathology* 83, 217-23.
- Apel K, Hirt H, 2004. Reactive oxygen species: metabolism, oxidative stress, and signal transduction. *Annual Review of Plant Biology* 55, 373-99.
- Arora A, Sairam RK, Srivastava GC, 2002. Oxidative stress and antioxidative system in plants. *Current Science* 82, 1227-38.
- CIMMYT, 2014. Maize Annual Report: Research Program on Maize. GGIAR. 48_p.
- Gorbe E, Calatayud A, 2012. Applications of chlorophyll fluorescence imaging technique in horticultural research: a review. *Scientia Horticulturae* 138, 24-35.
- Iqbal MJ, Goodwin PH, Leonardos ED, Grodzinski B, 2012. Spatial and temporal changes in chlorophyll fluorescence images of *Nicotiana benthamiana* leaves following inoculation with *Pseudomonas syringae* pv. *tabaci*. *Plant Pathology* 61, 1052-62.
- Jesus Junior WC, Vale FXR, Martinez CA, Coelho RR, Costa LC, Hau B, Zambolim L, 2001. Effects of angular leaf spot and rust on leaf gas exchange and yield of common bean (*Phaseolus vulgaris*). *Photosynthetica* 39, 603-06.
- Lamb C, Dixon RA, 1997. The oxidative burst in plant disease resistance. *Annual Review of Plant Physiology Plant Molecular Biology* 48, 251-75.
- Leonard KJ, Suggs EG, 1974. *Setosphaeria prolata* the ascigerous state of *Exserohilum prolatum*. *Mycologia* 66, 281-97.
- Luttrell ES, Bacon CW, 1977. Classification of *Myriogenospora* in the Clavicipitaceae. *Canadian Journal of Botany* 55, 20900-97.
- Medhy MC, 1994. Active oxygen species in plant defense against pathogens. *Plant Physiology* 105, 467-72.

Mittler R, 2002. Oxidative stress, antioxidants and stress tolerance. *Trends in Plant Science* 7, 405-10.

Munkvold GP, White DG, 2016. Compendium of corn diseases. 4rd Ed. St. Paul, MN, USA: The American Phytopathological Society.

Polidoros AN, Scandalios JG, 1999. Role of hydrogen peroxide and different classes of antioxidants in the regulation of catalase and glutathione-S-transferase gene expression in maize (*Zea mays* L.). *Physiology Plantarum* 106, 112-20.

Rolfe SA, Scholes JD, 2010. Chlorophyll fluorescence imaging of plant-pathogen interactions. *Protoplasma* 247, 163-75.

Sivanesan A, 1984. The bitunicate ascomycetes and their anamorphs. *Canadian Journal of Botany* 67, 1500-99.

Shtienberg D, 1992. Effects of foliar diseases on gas exchange processes: a comparative study. *Phytopathology* 82, 760-65.

CHAPTER 1

The Role of the Antioxidant Metabolism on Maize Leaves During the Infection Process of *Exserohilum turcicum*

Abstract

Northern leaf blight (NLB), caused by the fungus *Exserohilum turcicum* is one of the major foliar disease on maize. This study aimed to investigate the involvement of the antioxidative metabolism on the leaves of maize plants during the infection process of *E. turcicum*. This goal was achieved by examining the expression of genes (superoxide dismutase (*sod*), catalase (*cat*), ascorbate peroxidase (*apx*), peroxidase (*pox*), glutathione reductase (*gr*) and glutathione-S-transferase (*gst*)) and the activities of enzymes (superoxide dismutase (SOD), catalase (CAT), ascorbate peroxidase (APX), peroxidase (POX), glutathione reductase (GR), glutathione S-transferase (GST) and glutathione peroxidase (GPX)) involved in the antioxidant metabolism as well as determining the electrolyte leakage (EL) and the concentrations of malondialdehyde (MDA) and hydrogen peroxide (H₂O₂). The activities of SOD, CAT, APX, POX, GR, GST and GPX increased at 10 days after inoculation (dai) with *E. turcicum*. Relative expressions of the genes *sod*, *cat*, *apx*, *pox*, *gr* and *gst* were higher for the infected plants relative to non-infected plants mainly at advanced stages of fungal infection. In the infected leaves, the EL and the concentrations of MDA and H₂O₂ increased as the NLB symptoms developed on the maize leaves. In conclusion, a late participation of the antioxidative metabolism on the infected leaves was not helpful to counteract the deleterious effects of *E. turcicum* infection at its necrotrophic phase.

Introduction

Maize (*Zea mays* L.) is one of the main sources of carbohydrates and energy for food and feed besides having mainly applications in the industry in the industry (CIMMYT, 2014). Among the diseases affecting maize production, the northern leaf blight (NLB), caused by the fungus *Exserohilum turcicum* (Pass.) Leonard and Suggs (Anamorph) and *Setosphaeria turcica* (Luterell) Leonard and Suggs (teleomorph) (Leonard and Suggs, 1974; Luttrell and Bacon, 1977; Sivanesan, 1984), is one of the most important because can cause yield reduction greater than 50% when the plants are infected before the flowering period (Raymundo and Hooker, 1981; Munkvold and White, 2016). The epidemics of NLB occur in regions where the temperatures range from 18 to 27°C, with high relative humidity and low luminosity (Bentolila et al., 1991). The NLB symptoms start in the older leaves as elliptical lesions with necrotic center and chlorotic halos (With and Munkvold, 2016). The reactive oxygen species (ROS), such as the hydrogen peroxide (H₂O₂), the superoxide anion radical (O₂⁻) and the hydroxyl radical (OH[·]), are products of the normal plant cell metabolism that are constantly produced in low levels in the plasma membrane, peroxisomes, chloroplasts, mitochondria, cytoplasmic space and membrane-bound organelles of non-stressed plants (Das and Roychoudhury, 2014). However, under conditions of stress, such as the infection by pathogens, plants increase the production of ROS which are able to restrict the colonization of plant tissues by the pathogens or act as signaling molecules capable to induce host defense mechanisms (Torres et al., 2006; Wojtasek, 1997). However, high levels of ROS may also be cytotoxic and cause oxidative damage to the DNA molecules, proteins and lipids leading, therefore, to changes that cause cell death (Møller et al., 2007; Sharma et al., 2012). Increases in electrolyte leakage (EL) and in the concentration of malondialdehyde (MDA), which is a indicator of peroxidation of

the cell membrane lipids, increased in maize and rice plants infected by and *Stenocarpella macrospora* and *Monographella albescens*, respectively (Bermúdez-Cardona et al., 2015; Tatagiba et al., 2016). In order to regulate the production of ROS in the cells, the plants developed a ROS scavenging mechanism characterized by non-enzymatic and enzymatic antioxidant systems (Mittler, 2002; Apel and Hirt, 2004). The enzymatic antioxidant system involves several antioxidant enzymes such as the superoxide dismutase (SOD) which acts as the first line of defense for being responsible for the dismutation of O_2^- that results in the production of H_2O_2 and water while the catalase (CAT), ascorbate peroxidase (APX), peroxidase (POX) and glutathione peroxidase (GPX) are responsible for the detoxification of H_2O_2 (Alscher et al., 2002; Gill et al., 2015). The glutathione reductase (GR) and glutathione-S-transferase (GST) are involved in the detoxification process generating mainly reduced glutathione (GSH) which is a product of low molecular weight responsible for cleaning the ROS (Mullineaux and Rausch, 2005; Shahrtash, 2013; Das and Roychoudhury, 2014). The non-enzymatic antioxidant system involves compounds such as GSH, ascorbic acid (AA), α -tocopherol, carotenoids and flavonoids (Apel and Hirt, 2004; Das and Roychoudhury, 2014). Maize cultivars susceptible to *Stenocarpella macrospora* exhibited significant increase in the concentration of H_2O_2 as well as greater activities of SOD, CAT, APX, POX, GR, GPX and GST (Bermúdez-Cardona et al., 2015). High H_2O_2 concentration were associated with strong expression of the genes *cat 1*, *cat 2* and *gst* in maize plants showing, therefore, a role of H_2O_2 in the regulation of antioxidant genes (Polidoros and Scandalios, 1999). The expression of the genes coding for CAT, APX and GR as well as the activities of the enzymes produced by them increased in the leaves of maize plants sprayed with H_2O_2 (Zhang et al., 2007). The present study aimed to investigate the changes in the antioxidant metabolism of maize leaves during the

infection process of *E. turcicum* by examining the production of ROS as well as the expression of genes and the activities of the major enzymes involved in this process.

Materials and Methods

Plant growth

Maize seeds from cultivar P-1630 Hx susceptible to *E. turcicum*, were sown in plastic pots containing 2 kg of Tropstrato[®] (Vida Verde, Mogi Mirim, São Paulo, Brazil) substrate composed of a 1:1:1 mixture of pine bark, peat and expanded vermiculite. A total of 1.63 g of calcium phosphate monobasic was added to each plastic pot. A total of three seeds were sown per pot and at five days after seedlings emergence, each pot was thinned to two seedlings. Plants were kept in a greenhouse during the experiments (temperature $25 \pm 3^\circ\text{C}$ during the day and $21 \pm 2^\circ\text{C}$ at night, relative humidity $75 \pm 5\%$) and were fertilized weekly with 50 mL of a nutrient solution composed of 192 mg L^{-1} KCl, 104.42 mg L^{-1} K_2SO_4 , 150.35 mg L^{-1} MgSO_4 , 61 mg L^{-1} $\text{CH}_4\text{N}_2\text{O}$, 0.27 mg L^{-1} $\text{NH}_4\text{MO}_7\text{O}_{24}$, 1.61 mg L^{-1} H_3BO_3 , 6.67 mg L^{-1} ZnSO_4 , 1.74 mg L^{-1} CuSO_4 , 4.10 mg L^{-1} MnCl_2 , 4.08 mg L^{-1} FeSO_4 and 5.58 mg L^{-1} ethylenediaminetetraacetic acid (EDTA). The nutrient solution was prepared using deionized water. Plants were watered as needed.

Inoculum production and inoculation procedure

A monosporic isolate of *E. turcicum* ceded by the EPAGRI (Agricultural Research and Rural Extension Company of Santa Catarina) was grown in Petri dishes containing lactose casein hydrolyzed medium (Malca and Ullstrup, 1962) kept in an incubator (25°C and photoperiod of 16 hours light and 8 hours dark) for ten days. Plants were inoculated with a conidial suspension of *E. turcicum* (1×10^4 conidia/ml) at 30 days after

emergence (plants with five leaves fully expanded using a VL a Airbrush atomizer (Paassche Airbrush Co, Chicago, IL). Gelatin (1% w/v) was added to the suspension to aid conidial adhesion to the leaf blades. At the 8th day after plants inoculation, a total of 200 leaf fragments ($\approx 0.25 \text{ cm}^2$) containing disease symptoms were collected, disinfected in a solution of 70% (v/v) aqueous alcohol and 2% sodium hypochlorite solution (v/v) and transferred to Petri dishes (five leaf fragments per Petri dish) containing lactose casein hydrolyzed medium. Petri dishes were then transferred to an incubator (25°C and photoperiod of 16 hours of light and 8 hours of dark) for ten days. After this period, a total of 1 ml of sterile distilled water was added to each Petri dish and fungal mycelia were carefully disrupted using camel-hair brush in a laminar flow chamber in order to induce fungal sporulation. After this procedure, Petri dishes were again transferred to an incubator (25°C and photoperiod of 12 h with black light lamps emitting light near the ultraviolet (320-400 nm) and 12 hours dark)) during five days. Plants with five leaves fully expanded were inoculated with a conidial suspension of *E. turcicum* as described above and then kept in a growth chamber (temperature of $25 \pm 2^\circ\text{C}$ and relative humidity of $90 \pm 5\%$) under dark for the first 12 hours after inoculation in order to favor fungal infection. Thereafter, plants were transferred to a greenhouse (temperature of $25 \pm 2^\circ\text{C}$, relative humidity of $75 \pm 5\%$ and maximum natural photon flux density at plant canopy of $\approx 975 \mu\text{mol m}^{-2} \text{ s}^{-1}$) for the duration of the experiments.

Preparation of leaf samples for light microscopy

Leaf fragments ($\approx 4 \text{ mm}^2$) with symptoms of NLB were collected at 20 dai. The fragments were placed in glass vials, fixed with 2.5% glutaraldehyde in 0.1 M sodium cacodylate buffer (pH 7.2) during 48 h, dehydrated in an ethanol series and infiltrated in historesin methacrylate (Historesin Leica[®]). A total of three blocks containing two leaf

fragments were used to obtain the sections (3 μm thick) with the help of a rotary microtome auto-advance model RM 2255 (Leica Microsystems Inc., Deerfield, IL, USA). The sections were stained with toluidine blue 0.05% (pH 4.7) and observed in a Carl Zeiss Axio Imager A1 microscopy (Carl Zeiss, Germany) with Digital Camera Spot Insight_{colour} 3.2.0 (Diagnostic Instruments Inc, Merrick, NY, USA).

Determination of enzymes activities

For all biochemical analyses, leaf samples were collected from the second, third and fourth leaves fully expanded, from the base to the top, of non-inoculated and inoculated plants at 5, 10, 15 and 20 dai. Leaf samples were kept in liquid nitrogen during sampling and then stored at -80°C for further analysis.

In order to obtain the leaf extract to determine the activities of the enzymes superoxide dismutase (SOD, EC 1.15.1.1), catalase (CAT, EC 1.11.1.6), ascorbate peroxidase (APX, EC 1.11.1.11), peroxidase (POX, EC 1.11.1.7), glutathione reductase (GR, EC 1.8.1.7), glutathione-S-transferase (GST, EC 2.5.1.18) and glutathione peroxidases (GPX, EC 1.11.1.9), a total of 0.3 g of leaf fragments were macerated in liquid nitrogen (N_2) in a mortar to obtain a fine powder. The obtained powder was homogenized in 2 ml of potassium phosphate buffer 0.5 M (pH 6.8) containing 0.1 M ethylenediaminetetraacetic acid (EDTA), 0.1% Triton X-100, 3 Mm DL-dithiothreitol (DTT) and 1% (w/v) polyvinylpyrrolidone (PVP). The homogenate was centrifuged at $12.000 \times g$ for 15 min at 4°C and the supernatant was divided into aliquots which were used as extract for the enzymatic determinations. SOD activity was determined by adding 20 μL of leaf extract in 980 μL of reaction mixture containing 50 mM sodium phosphate buffer (pH 7.8), 13 mM methionine, 75 μM *p*-nitro blue tetrazolium (NBT) 75 μM , 0.1 mM EDTA and 2 μM riboflavin (Del Longo et al., 1993). The reaction of

samples occurred at 25° C under illumination lamps of 15 W. After 10 minutes of exposure to light, illumination was stopped and the blue formazan produced by photoreduction of NBT was measured in a spectrophotometer using the 560 nm absorbance (Giannopolitis and Ries, 1977). The absorbance at 560 nm of a reaction mixture with the same composition, but kept in the dark for 10 min, served as a blank. One unit of SOD was defined as the amount of enzyme necessary to inhibit NBT photoreduction by 50%. CAT activity was determined by the method of Cakmak and Marschner (1992). The reaction was started by adding 50 µL of leaf extract in 950 µL of reaction mixture containing 50 mM sodium phosphate buffer (pH 7.8) and 100 mM H₂O₂. The decrease in absorbance was determined by consumption of H₂O₂ at 240 nm for 1 min. The molar extinction coefficient of 36 mM⁻¹ cm⁻¹ was used to calculate CAT activity (Anderson et al., 1995). APX activity was determined by the method of Nakano and Asada (1981). The reaction was started by adding 20 µL of leaf extract in 980 µL of reaction mixture containing 50 mM potassium phosphate buffer (pH 6.8), 1 mM H₂O₂ and 0.8 mM sodium ascorbate. The decrease in absorbance was measured by oxidation of ascorbate at 290 nm for 1 min. The molar extinction coefficient of 2.8 mM⁻¹ cm⁻¹ was used to calculate APX activity. POX activity was determined by the method of Kar and Mishra (1976). The reaction was started by adding 20 µL of leaf extract in 980 µL of reaction mixture containing 25 mM potassium phosphate buffer (pH 6.8), 20 mM pyrogallol and 20 mM H₂O₂. The increase in absorbance was determined by oxidation of pyrogallol and consumption of H₂O₂ at 420 nm for 1 min. The molar extinction coefficient of 2.47 mM⁻¹ cm⁻¹ was used to calculate POX activity (Chance and Maehley, 1955). GR activity was determined by adding 100 uL of leaf extract in 900 µL of a reaction mixture consisting of 100 mM potassium phosphate buffer (pH 7.5), 1 mM EDTA, 1 mM oxidized glutathione (GSSG) and 0.1 mM NADPH prepared in 0.5 mM

Tris-HCl buffer (pH 7.5) (Carlberg and Mannervik, 1985). The decrease in absorbance was measured at 340 nm for 1 min. The molar extinction coefficient of $6.22 \text{ mM}^{-1} \text{ cm}^{-1}$ was used to calculate GR activity (Foyer and Halliwell, 1976). GST activity was determined by the methodology of Habig et al. (1974). The reaction was started by adding 20 μL of leaf extract in 980 μL of reaction mixture containing 97 mM potassium phosphate buffer (pH 6.5), 0.97 mM EDTA, 2.5 mM reduced glutathione (GSH) and 1.0 mM 1-chloro-2,4-dinitrobenzene. The absorbance was measured at 340 nm for 1 min. The extinction coefficient of $9.6 \text{ mM}^{-1} \text{ cm}^{-1}$ was used to calculate GST activity. GPX activity was determined by adding 115 μL of leaf extract in 885 μL of a reaction mixture consisting of 50 mM potassium phosphate buffer (pH 7.0), 1 mM EDTA, 0.114 M NaCl, 1 mM GSH, 0.2 mM NADPH, 0.25 H_2O_2 and 1 mM of glutathione reductase unit (Nagalakshmi and Prasad, 2001). The decrease in absorbance was measured at 340 nm for 1 min. The molar extinction coefficient of $6.22 \text{ mM}^{-1} \text{ cm}^{-1}$ was used to calculate GPX activity (Anderson and Davis, 2004). Protein concentration was measured using the Bradford assay with bovine serum albumin as a standard (Bradford, 1976).

Determination of hydrogen peroxide (H_2O_2) concentration

A total of 0.2 g of leaf tissue was macerated in liquid N_2 in a mortar to obtain a fine powder. The obtained powder was homogenized in 2 ml consisting of 50 mM potassium phosphate buffer (pH 6.5) and 1 mM hydroxylamine. The homogenate was centrifuged at $10,000 \times g$ for 15 min at 4°C (Kuo and Kao, 2003). The reaction was started by adding 100 μL of the supernatant in 1.9 mL of reaction mixture containing of 100 μM $\text{FeNH}_4(\text{SO}_4)$, 25 mM sulfuric acid, 250 μM xylenol orange and 100 mM sorbitol (Gay and Gerbicki, 2000). Samples were kept in the dark for 30 min and the absorbance determined at 560 nm. The controls of the reagent and leaf extracts were prepared in

parallel and subtracted from the sample. A standard curve of H₂O₂ (Sigma-Aldrich, São Paulo, Brazil) was used to determine the H₂O₂ concentration.

Determination of malondialdehyde (MDA) concentration

The MDA concentration was determined according to the method of Cakmak and Horst (1991) with a few modifications. A total of 0.2 g of leaf tissue was macerated in liquid N₂ in a mortar to obtain a fine powder. The obtained powder was homogenized in 2 ml of a solution of trichloroacetic acid (TCA) 1% (w/v). The homogenate was centrifuged at 12.000 × g for 15 min at 4°C. After centrifugation, 0.5 ml of the supernatant was added to 1.5 ml of 0.5% thiobarbituric acid (TBA) solution (w/v) (prepared in 20% (w/v) TCA) and incubated in a water bath at 95°C for 30 min. After this period, the reaction was quenched in an ice bath. Samples were centrifuged at 9000 × g for 10 min and the specific absorbance of the supernatant was determined at 532 nm. Non specific absorbance was measured at 600 nm and subtracted from the value of the specific absorbance. The extinction coefficient of 155 mM⁻¹ cm⁻¹ was used to calculate the MDA concentration (Heath and Packer, 1968).

Determination of electrolyte leakage (EL)

The EL was determined by method of Lima et al. (2002) with some modifications. A total of 20 leaf discs (8 mm in diameter) were collected from the third leaf from the base to the top, of each plant per replication of each treatment at 5, 10, 15 and 20 dai. Leaf discs were washed in deionized water immediately after being sampled and placed in glass vials containing 60 mL of distilled water. After 4 hours at 25°C, reading of the first conductivity was performed. Leaf discs were immersed in distilled water and then

submitted to heating (90°C for 2 h). After this period, a new conductivity reading was performed using a conductivity meter (Tecnoon mCA-150; MS Tecnoon Instrumentação Científica, São Paulo, Brazil). The EL was expressed as the percentage of the total conductivity.

RNA extraction and real time quantitative PCR (RT-qPCR)

Leaf samples were collected from the second, third and fourth leaves fully expanded, from the base to the top, of non-inoculated and inoculated plants at 5, 10, 15 and 20 dai. Samples were kept in liquid N₂ during sampling and then stored at -80°C for further analysis. Leaf samples from non-inoculated and inoculated plants were ground to powder under liquid N₂ for RNA extraction using the RNAqueous[®] kit (Applied Biosystems, Foster City, USA) according to the manufacturer's instructions. After extraction, the total RNA concentration was determined using a Nanodrop ND-1000 spectrophotometer (Nanodrop Technologies, Rockland, USA) and RNA quality was assessed by the integrity of the bands of ribosomal RNA on agarose gel 1.5%. The RNA purity was determined by the ratio of absorbance at 260 and 280 nm. Next, total RNA was treated with RNase Free DNase (Promega, São Paulo, Brazil) according to the manufacturer's recommendations. Total RNA of the samples was again quantified and evaluated for integrity as previously described. First-strand cDNA was synthesized using 1 µg of total RNA, M-MLV reverse transcriptase (Invitrogen, São Paulo, Brazil) and the primer oligo (dT) 12-18 (Sigma-Aldrich, São Paulo, Brazil) according to the manufacturer's instructions. The genes analyzed, the sequences of designed primers and the sequences of RT-qPCR primers are listed in Table 1. Primers sequences for the amplification of the *glutathione-S-transferase* (*gst*) and *catalase* (*cat*) genes were obtained according to Hermes et al. (2013) and the primer sequences for the genes

superoxide dismutase (sod), *peroxidase (pox)*, *ascorbate peroxidase (apx)* and *glutathione reductase (gr)* were confirmed in accordance with the sequences deposited in GenBank (<http://www.ncbi.nlm.nih.gov/>). Relative quantification of gene transcripts was carried out using the method $2^{-\Delta\Delta Ct}$ (Livak and Schmittgen, 2001). The accumulation of transcripts for each gene was normalized using the expression of the constitutive genes *glyceraldehyde-3-phosphate dehydrogenase (gapdh)*. The RT-qPCR reactions to determine the expression of *cat* and *apx* genes were composed of a mixture containing 10 μ L of 2 \times SYBR-green master PCR mix (Applied Biosystems, São Paulo, Brazil), 0.4 μ l of primers, 5 μ l of cDNA (20 ng) and 4.6 μ l of water. In order to determine the expression of the *gr*, *sod* and *gst* genes, the reaction mixture contained 10 μ L of 2 \times SYBR-green master PCR mix (Applied Biosystems, São Paulo, Brazil), 1.2 μ l of primers, 5 μ l of cDNA (20 ng) and 3.8 μ l of water. The RT-qPCR reaction to determine the expression of *pox* was composed of 10 μ L of 2 \times SYBR-green master PCR mix (Applied Biosystems, São Paulo, Brazil), 1.6 μ l of primers, 5 μ l of cDNA (20 ng) and 3.4 μ l of water. The amplification conditions were two stages of 50°C for 2 min and 95°C for 10 min followed by 40 cycles at 95 and 60°C, respectively, for 30 s each. The dissociation curve was observed after amplification to ensure that only a single amplicon was produced in each reaction. Amplification of the specific regions of targeted genes and the real-time detection of amplicon production was undertaken in a CFX96 Real-Time PCR Detection System (Bio-Rad Laboratories, Inc., São Paulo, Brazil).

Experimental design and statistical analysis

Two experiments (Experiments 1 and 2) was arranged in a completely randomized with four replications to evaluate NLB severity and to obtain the leaf samples for the light microscopy. Two other experiments (Experiments 3 and 4), consisting of two treatments

(non-inoculated and inoculated plants), was arranged in a completely randomized with four replications to obtain the leaf samples for the biochemical analysis. Each experimental unit corresponded to a plastic pot containing two plants. Data from NLB severity from experiments 1 and 2 and from the biochemical variables from experiments 3 and 4 were analyzed the MIXED procedure of the SAS software (Release 8.02 Level 02M0 for Windows, SAS Institute, Inc., 1989, Cary, NC, USA) to determine if data from these experiments could be combined (Moore and Dixon, 2015). For all variables evaluated on experiments 3 and 4, the ANOVA was considered 2×4 factorial experiment consisting of non-inoculated and inoculated plants (plant inoculation (PI) and four sampling time (ST)). Data from all variables were analyzed by ANOVA and means from the treatments were compared with the *F*-test using SAS (version 6.12; SAS Institute, Inc., Cary, NC). Data from each variable were correlated among them using Pearson correlation.

Results

Northern leaf blight symptoms and leaf tissue colonization by *E. turcicum*

Symptoms of northern leaf blight on maize leaves were characterized as elliptical lesions with their center necrotic and with chlorotic halos (Fig. 1A) and fungal hyphae colonized mainly the xylem vessels (Fig. 1B).

Enzyme activities

The factor PI was significant for the activities of the enzymes SOD, CAT, APX, POX, GR, GPX and GST and the factor ST was not significant only for GST. The interaction PI \times ST was significant only for APX activity (Table 2). There were significant

increases of 60, 54 and 51% for SOD activity (Fig. 2A), of 43, 65 and 69% for APX activity (Fig. 2C), of 68, 58 and 49% for POX activity (Fig. 2D) and of 42, 25 e 49% for GR (Fig. 2E), respectively, at 10, 15 and 20 dai for inoculated plants in comparison to the non-inoculated ones. There were significant increases of 34, 33 and 41% for CAT activity (Fig. 2B), respectively, at 5, 10 and 20 dai for inoculated plants in comparison to non-inoculated ones. There were significant increases of 58 and 39% for GST and GPX activities (Fig. 2F and G), respectively, at 20 dai for inoculated plants in comparison to the non-inoculated ones.

Concentrations of H₂O₂ and MDA and determination of EL

The factor PI was significant for the concentration of H₂O₂, MDA and EL and the factor ST and the interaction PI × ST were significant only for EL. There were significant increases of 22 and 25% for the H₂O₂ concentration (Fig. 3A) and of 30 e 21% for MDA concentration (Fig. 3B), respectively, at 15 and 20 dai for inoculated plants in comparison to non-inoculated ones. There were significant increases of 47, 37 and 45% for EL, respectively, at 10, 15 and 20 dai for inoculated plants in comparison to the non-inoculated ones (Fig. 3C).

Genes expression

The expression of all genes were higher for the inoculated plants when relativized to the non-inoculated plants. For inoculated plants, *sod* expression increased by 1.03, 1.23, 1.97 and 6.57 folds at 5, 10, 15 and 20 dai, respectively, in relation the non-inoculated plants (Fig. 5A). The *cat* expression was 1.84, 4.70, 4.01 and 8.11 folds increased for inoculated plants in comparison to non-inoculated plants at 5, 10, 15 and 20 dai, respectively (Fig. 5B). The *apx* expression was 1.06, 1.38, 1.86 and 3.03 folds increased

for inoculated plants comparison to non-inoculated plants at 5, 10, 15 and 20 dai, respectively (Fig. 5C). For inoculated plants, the *pox* expression increased by 2.88, 8.03, 5.79 and 6.60 folds at 5, 10, 15 and 20 dai, respectively, in comparison to the non-inoculated plants (Fig. 5D). The *gr* expression was 1.04, 1.52, 1.93 and 4.17 folds increased for inoculated plants in comparison to non-inoculated plants at 5, 10, 15 and 20 dai, respectively (Fig. 5E). The *gst* expression was 6.01, 4.53, 16.08 and 22.08 folds increased for inoculated plants in comparison to non-inoculated plants at 5, 10, 15 and 20 dai, respectively (Fig. 5F).

Pearson correlation

SOD activity was positively correlated with the activity of all other enzymes. CAT activity was negatively correlated with APX activity and positively with the other enzymes. APX activity was also negatively correlated with GPX activity and positively correlated with the others enzymes. POX activity was negatively correlated only with GST activity. GR activity was positively correlated with all other enzymes and GST and GPX were negatively correlated each other. Northern leaf blight severity was positively correlated with all enzymes, with the exception of GST and GPX. H₂O₂ concentration was positively correlated with NLB severity as well as with SOD, CAT and POX activities and negatively correlated with APX, GR, GST and GPX activities. MDA concentration correlated positively with NLB severity, GST and GPX activities and H₂O₂ concentration. The NLB severity, the activity of all enzymes and MDA and H₂O₂ concentration were positively correlated with EL (Table 3).

Discussion

The present study provides novel information regarding the biochemical and molecular changes in the antioxidant metabolism in the leaves of maize plants during the infection process of *E. turcicum*. The activation of the antioxidant metabolism of maize leaves was particularly evident at advanced stages of fungal infection. At both 15 and 20 dai, high concentration of H₂O₂ was noticed in the infected leaves which may serve as signal molecules that caused the greater expression of genes involved in the antioxidant metabolism and, consequently, higher activities of the enzymes produced by them. The greater production of H₂O₂ at advanced stage of *E. turcicum* infection can possibly be associated with its life style. It is known that *E. turcicum* is a hemibiotrophic fungus behaving as a biotrophic at early stages of infection and become necrotrophic after gaining full access to the host tissue (Jennings and Ullstrup, 1957). According to Muiru et al. (2008), the germination of conidia from different isolates of *E. turcicum* occurred from 15 to 20 hours after plant inoculation and appressorium formation at 24 hours after inoculation. However, the authors failed to provide information on the exact time which the fungus starts its necrotrophic stage. By contrast, for the sorghum *Colletotrichum sublineolum* interaction, the biotrophic phase begins with the formation of vesicles and the first infection hyphae within the first penetrated epidermal cell while the necrotrophic phase occurs when the fungus colonizes the adjacent cells (Warton et al., 2001). Many necrotrophic pathogens can take advantage of the H₂O₂ production because of the availability of nutrients in the death cells. Govrin and Levine (2000) reported that the inoculation of *Arabidopsis* plants with *Botrytis cinerea* induced an oxidative burst with high production of H₂O₂ that facilitated the colonization of host tissues by pathogen. The necrotrophic pathogens *Rhynchosporium secalis* and *Pyrenophora teres* also benefited from the great H₂O₂ production in the barley leaves

(Able, 2003). In contrast to what have been reported for the necrotrophic pathogens, the ROS, mainly the H₂O₂, restricted the colonization of wheat leaves by the biotrophic fungus *Puccinia striiformis* f. sp. *tritici* (Wang et al., 2007). Barna et al. (2012) reported that the wheat plants exposed to heat became more susceptible to rust due to an increase in CAT activity that contributed to reduce the concentration of H₂O₂ confirming, therefore, that low levels of ROS were important at early stage of the development of biotrophic pathogens. In the present study, there was a high CAT activity at 5 dai for the infected plants in comparison to the non-infected ones contributing, therefore, for the maintenance of low levels of H₂O₂ that possibly may have been generated during the early stages of *E. turcicum* infection. In the compatible interaction wheat-*Septoria tritici* there was low H₂O₂ accumulation during the biotrophic phase of the fungus which lasted up to 11 dai. However, at 13 dai there was an increase in the H₂O₂ production which was associated with the collapse of the leaf cells and the visible disease symptoms characterizing, therefore, the necrotrophic phase of the pathogen (Shetty et al., 2003). This finding is supported by the results of the present study which showed a greater H₂O₂ production only at 15 and 20 dai. At these times, the necrotic lesions were evident on the maize leaves and at 20 dai massive fungal mycelia were noticed in the xylem vessels. Furthermore, the NLB severity was positively correlated with H₂O₂ production. The H₂O₂ production was also followed by an increase in the EL at 10 dai and great MDA concentration from 10 to 15 dai indicating, therefore, the harmful effect of H₂O₂ to the cell membranes that may be intensified by the release of non-host selective toxins by *E. turcicum*. Gal et al. (2000) found a positive correlation between a high permeability of the cell membranes and the concentration of non-selective toxins produced by *E. turcicum*. Leaves of maize plants infected by *S. macrospora* showed higher H₂O₂ and MDA concentration and an increase in the EL (Bermúdez-Cardona et

al., 2015). In the present study, it is important to note that a greater EL as well as high MDA and H₂O₂ concentrations were associated with the development of NLB. In general, the expression of genes and the activities of enzymes involved in the antioxidant metabolism were higher for the infected plants in comparison the non-infected ones from 10 dai until advanced stages of fungal infection. The SOD activity was higher from 10 dai until advanced stages of fungal infection confirming suggested, therefore, the low ROS production during the biotrophic phase of *E. turcicum*. The expression of the *sod* genes was up regulated in the infected plants in comparison to the non-infected plants ones mainly from 10 dai and reached its high expression at 20 dai. The CAT activity was higher at 5 dai in the infected plants in comparison to the non-infected plants ones at both 10 and 20 dai. The expression of *cat* gene was also up regulated throughout the infectious process of *E. turcicum* in the infected plants than in the non-infected ones mainly 20 dai. The APX, GPX, POX and CAT are responsible for the removal of H₂O₂ at different locations in the cell. The CAT operates predominantly in peroxisomes and mitochondria; the APX performs the removal of H₂O₂ present in both cytosol and chloroplast; the POX acts in the cell walls and vacuoles and the GPX performs its activity at the cytosol, vacuole and cell walls (Sharma et al., 2012; Das and Roychoudhury, 2014). Both APX a and POX showed an increase on their activities in the infected plants the infected plants from 10 dai corresponding, therefore, to a time where the H₂O₂ production was high corresponding to an advanced stage of fungal infection. The GPX also played an important role in response to an increase in the H₂O₂ concentration mainly at 20 dai. The GR participates in the ascorbate-glutathione cycle and is important in the generation of GSH, a compound that is involved in the scavenging of ROS (Das and Roychoudhury, 2014). The GR activity was high in infected plants from 10 to 20 dai. In comparison to GR, the GST is also responsible for

the generation of GSH and in the present study its activity was higher for infected plants only at 20 dai. The expression of the *gr* gene was up-regulated in the infected plants mainly at 20 dai and the greatest expression of the *gst* gene occurred at both 15 and 20 dai for infected plants in comparison to the non-infected ones. The greater expression of genes and an increase in the activities of the enzymes involved in the antioxidant metabolism are consistent with the increase in the H₂O₂ production and corroborates with the fact that the H₂O₂ is involved in the activation of host defense and also in the antioxidative metabolism (Mittler et al., 2004; Scandalios, 2005). The exposure of leaves of maize plants to lower concentrations of H₂O₂ in contrast to high concentration resulted in low transcript levels for the genes *cat 1*, *cat 3* and *gst 1* (Polidoros and Scandalios, 1999). Zhang et al. (2007) reported that the treatment of leaves of maize plants with H₂O₂ resulted in an increase on the expression of the genes *cat 1*, *apx* and *gr 1* and in the activities of CAT, GR, SOD and APX. In the present study, it is plausible to postulate that the great expression of genes and activities of enzymes involved in the antioxidative metabolism were of detrimental role in the removal of H₂O₂. According to Bermúdez-Cardona et al. (2015), there was a gradual increase in H₂O₂ concentration on maize leaves throughout the infection process of *S. macrospora* while the activities of the enzymes involved in the antioxidative metabolism were higher at the beginning of fungal infection and decreased thereafter. By contrast, in the present study a great H₂O₂ production occurred mainly at the advanced stage of fungal infection and was accompanied by an increase in both expression of genes and activities of enzymes involved in the antioxidative metabolism. The lifestyle of *E. turcicum* may also have contributed to the accumulation of H₂O₂ in the infected cells when we consider that at this time the fungus already reached its necrotrophic phase. In conclusion, the metabolism triggered by the generation of H₂O₂ was not efficient to counteract the

deleterious effects of *E. turcicum* infection on maize leaves mainly at its necrotrophic phase.

References

- Able AJ, 2003. Reactive oxygen during plant fungal necrotroph interactions. *Protoplasma* 221, 137-43.
- Alscher RG, Erturk N, Heath LS, 2002. Role of superoxide dismutases (SODs) in controlling oxidative stress in plants. *Journal of Experimental Botany* 53, 1331-41.
- Anderson D, Prasad K, Stewart R, 1995. Changes in isozyme profiles of catalase, peroxidase and glutathione reductase during acclimation to chilling in mesocotyls of maize seedlings. *Plant Physiology* 109, 1247-57.
- Anderson JV, Davis DG, 2004. Abiotic stress alters transcript profiles and activity of glutathione S-transferase, glutathione peroxidase, and glutathione reductase in *Euphorbia esula*. *Plant Physiology* 120, 421-33.
- Apel K, Hirt H, 2004. Reactive oxygen species: metabolism, oxidative stress, and signal transduction. *Annual Review of Plant Biology* 55, 373-99.
- Barna B, Fodor J, Harrach BD, Pogány M, Kiraly Z, 2012. The Janus face of reactive oxygen species in resistance and susceptibility of plants to necrotrophic and biotrophic pathogens. *Plant Physiology and Biochemistry* 59, 37-43.
- Bentolila S, Guitton C, Bouvet N, Sailand A, Nykaza S, Freyssinet, 1991. Identification of RFLP marker tightly linked to the Ht1 gene in maize. *Theoretical Applied Genetics* 82, 393-98.
- Bermúdez-Cardona MB, Bispo WMS, Rodrigues FA, 2015. Physiological and biochemical alterations on maize leaves infected by *Stenocarpella macrospora*. *Acta Physiologiae Plantarum* 37, 1-17.

Bradford MN, 1976. A rapid and sensitive method for the quantitation of microgram quantities of protein utilizing the principle of protein-dye binding. *Analytical Biochemistry* 72, 248-54.

Cakmak I, Horst WJ, 1991. Effect of aluminum on lipid peroxidation, superoxide dismutase, catalase, and peroxide activity in root tip of soybean (*Glycine max*). *Physiologia Plantarum* 83, 463-68.

Cakmak I, Marschner H, 1992. Magnesium deficiency and high light intensity enhance activities of superoxide dismutase, ascorbate peroxidase and glutathione reductase in bean leaves. *Plant Physiology* 98, 1222-27.

Carlberg C, Mannervik B, 1985. Glutathione reductase. *Methods Enzymology* 113, 488-95.

Chance B, Maehley AC, 1955. Assay of catalases and peroxidases. *Methods Enzymology* 2, 764-75.

CIMMYT, 2014. Maize Annual Report: Research Program on Maize. GGIAR. 48p.

Das K, Roychoudhury A, 2014. Reactive oxygen species (ROS) and response of antioxidants as ROS-scavengers during environmental stress in plants. *Frontiers in Environmental Science* 2, 1-13.

Del Longo OT, González CA, Pastori GM Trippi, 1993. Antioxidant defenses under hyperoxygenic and hyperosmotic conditions in leaves of two lines of maize with differential sensitivity to drought. *Plant Cell Physiology* 34, 1023-28.

Foyer CH, Halliwell B, 1976. The presence of glutathione and glutathione reductase in chloroplasts: a proposed role in ascorbic acid metabolism. *Planta* 133, 21-5.

Gao DJ, Min HJ, Juan YS, 2000. The effect of HT-toxin produced by *Exserohilum turcicum* on membrane leakage of corn. *Journal of Agricultural University of Hebe* 3, 3980-98.

Gay C, Gerbicki JM, 2000. A critical evaluation of sorbitol on the ferric-xylenol orange hydroperoxide assay. *Analytical Biochemistry* 284, 217-22.

Giannopolitis CN, Ries SK, 1977. Superoxide dismutases: I. occurrence in higher plants. *Plant Physiology* 59, 309-14.

Gill SS, Anjum NA, Gill R, Hasanuzaman M, Fujita M, Misha P, Sabat SC, Tujeta N, 2015. *Environmental Science and Pollution Research* 22, 10375-94.

Govrin EM, Levine A, 2000. The hypersensitive response facilitates plant infection by the necrotrophic pathogen *Botrytis cinerea*. *Current Biology* 10, 751-57.

Habig WH, Pabst MJ, Jakoby WB, 1974. Glutathione-S-transferases: the first enzymatic step in mercapturic acid formation. *Journal Biology Chemistry* 249, 7130-39.

Heath RL, Packer L, 1968. Photoperoxidation in isolated chloroplast: I. Kinetics and stoichiometry of fatty acid peroxidation. *Archives Biochemistry and Biophysics* 125, 189-98.

Hermes VS, Dall'Asta P, Amaral FP, Anacleto KB, Arise ACM, 2013. The regulation of transcription of genes related to oxidative stress and glutathione synthesis in *Zea mays* leaves by nitric oxide. *Biologia Plantarum* 57, 620-26.

Jennings PR, Ullstrup AJ, 1957. A histological study of three *Helminthosporium* leaf blights of corn. *Phytopathology* 47, 707-14.

Kar M, Mishra D, 1976. Catalase, peroxidase, and polyphenoloxidase activities during rice leaf senescence. *Plant Physiology* 57, 315-19.

Kuo MC, Kao CH, 2003. Aluminium effects on lipid peroxidation and antioxidative enzyme activity in rice leaves. *Biologia Plantarum* 46, 149-52.

Lima ALS, DaMatta FM, Pinheiro HA, Totola MR, Loureiro ME, 2002. Photochemical response and oxidative stress in two clones of *Coffea canephora* under water deficit conditions. *Environmental and Experimental Botany* 47, 239-24.

- Livak KJ, Schmittgen TD, 2001. Analysis of relative gene expression data using real-time quantitative PCR and the method $2^{-\Delta\Delta C_t}$. *Methods* 25, 402-08.
- Leonard KJ, Suggs EG, 1974. *Setosphaeria prolata* the ascigerous state of *Exserohilum prolatum*. *Mycologia* 66, 281-97.
- Luttrell ES, Bacon CW, 1977. Classification of *Myriogenospora* in the Clavicipitaceae. *Canadian Journal of Botany* 55, 20900-97.
- Malca I, Ullstrup AJ, 1962. Effects of carbon and nitrogen nutrition on growth and sporulation of two species of *Helminthosporium*. *Bulletin Torrey Botanical Club* 89, 240-49.
- Mittler R, 2002. Oxidative stress, antioxidants and stress tolerance. *Trends in Plant Science* 7, 405-10.
- Mittler R, Vanderauwera S, Gollery M, Van Breusegem F, 2004. Reactive oxygen gene network of plants. *Trends in Plant Science* 9, 490-98.
- Møller IM, Jensen PE, Hansson A, 2007. Oxidative modifications to cellular components in plants. *Annual Review of Plant Biology* 58, 459–81.
- Moore KJ, Dixon P. Analysis of Combined Experiments Revisited, 2015. *Agronomy Journal* 107, 763-71.
- Muiru WM, Mutitu EW, Kimenju JW, Koopmann B, Tiedemann AV, 2008. Infectious structures and response of maize plants to invasion by *Exserohilum turcicum* in compatible and incompatible host pathogen systems. *Journal of Applied Biosciences* 10, 532-37.
- Mullineaux PM, Rausch T, 2005. Glutathione, photosynthesis and the redox regulation of stress-responsive gene expression. *Photosynthesis Research* 86, 459-74.
- Munkvold GP, White DG. Compendium of corn diseases. 4th Ed. St. Paul, MN, USA: The American Phytopathological Society.

- Nagalakshmi N, Prasad MNV, 2001. Responses of glutathione cycle enzymes and glutathione metabolism to copper stress in *Scenedesmus bijugatus*. *Plant Science* 160 291-99.
- Nakano Y, Asada K, 1981. Hydrogen peroxide is scavenged by ascorbate-specific peroxidase in spinach chloroplasts. *Plant Cell Physiology* 22, 867-80.
- Polidoros AN, Scandalios JG, 1999. Role of hydrogen peroxide and different classes of antioxidants in the regulation of catalase and glutathione-S-transferase gene expression in maize (*Zea mays* L.). *Physiology Plantarum* 106, 112-20.
- Raymundo AD, Hooker AL, 1981. Measuring the relationship between northern corn leaf blight and yield losses. *Plant Disease* 65, 325-27.
- Scandalios JG, 2005. Oxidative stress: molecular perception and transduction of signals triggering antioxidant gene defenses. *Brazilian Journal of Medical and Biological Research* 38, 995-1014.
- Shahrtash M, 2013. Plant glutathione-S-transferases function during environmental stresses: A review article. *Plant Biology* 58, 19-25.
- Sharma P, Jha AB, Dubey RS, Pessarakly M, 2012. Reactive oxygen species, oxidative damage, and antioxidative defense mechanism in plants under stressful conditions. *Journal of Botany* 10155/2012/217037.
- Shetty NP, Kristensen BK, Newman MA, Møller, Gregersen PL, Jørgensen HJL, 2003. Association of hydrogen peroxide with restriction of *Septoria tritici* in resistant wheat. *Physiological and Molecular Plant Pathology* 62, 333-46.
- Sivanesan A, 1984. The bitunicate ascomycetes and their anamorphs. *Canadian Journal of Botany* 67, 1500-99.

- Tatagiba SD, Neves FW, Bitti ALFE, Rodrigues FA, 2016. Changes in gas exchange and antioxidant metabolism on rice leaves infected by *Monographella albescens*. *Topical Plant Pathology* 41, 33-41.
- Torres MA, Jones JDG, Dangi JL, 2006. Reactive oxygen species signaling in response to pathogens. *Plant Physiology* 141, 373-78.
- Vieira RA, Mesquini RM, Silva CN, Hata FT, Tessmann DJ, Scapim CA, 2014. A new diagrammatic scale for the assessment of northern corn leaf blight. *Crop Protection* 56, 55-7.
- Zhang A, Jiang M, Zhang J, Ding H, Xu S, Hu X, Tan M, 2007. Nitric oxide induced by hydrogen peroxide mediates abscisic acid-induced activation of the mitogen-activated protein kinase cascade involved in antioxidant defense in maize leaves. *New Phytologist* 175, 36-50.
- Wang CF, Huang LL, Buchenauer H, Han QM, Zhang HC, Kang ZS, 2007. Histochemical studies on the accumulation of reactive oxygen species (O₂ and H₂O₂) in the incompatible and compatible interaction of wheat-*Puccinia striiformis* f.sp. *tritici*. *Physiological and Molecular Plant Pathology* 71, 230-39.
- Wharton PS, Julian AM, O'Connell RJ, 2001. Ultrastructure of the infection of *Sorghum bicolor* by *Colletotrichum sublineolum*. *Phytopathology* 91, 149-58.
- Wojtasek P, 1997. Oxidative burst: an early plant response to pathogen infection. *Biochemistry Journal* 322, 681-92.

List of Tables and Figures

Table 1. Genes and primers sequences of the genes involved in the antioxidant metabolism analyzed using quantitative reverse transcription PCR, in the leaves of maize plants non-inoculated or inoculated with *Exserohilum turcicum*.

Table 2. Analysis of variance of the effects of sampling times (ST), plant inoculation (PI) as well as the interaction (ST × PI) on activities of superoxide dismutase (SOD), catalase (CAT), ascorbate peroxidase (APX), peroxidase (POX), glutathione reductase (GR), glutathione-S-transferase (GST), glutathione peroxidase (GPX), concentrations of hydrogen peroxide (H₂O₂) and malondialdehyde (MDA) as well as electrolyte leakage (EL).

Table 3. Pearson correlation coefficients among northern leaf blight severity (Sev), activities of superoxide dismutase (SOD), catalase (CAT), ascorbate peroxidase (APX), peroxidase (POX), glutathione reductase (GR), glutathione-S-transferase (GST), glutathione peroxidase (GPX), concentrations of hydrogen peroxide (H₂O₂) and malondialdehyde (MDA) as well as electrolyte leakage (EL (%)) determined in the leaves maize plants inoculated with *Exserohilum turcicum*.

Figure 1. Symptoms of northern leaf blight (A) and light micrograph of a longitudinal leaf section (B) at 20 days after inoculation of maize plants with *Exserohilum turcicum*. Arrows indicate the xylem vessels colonized by fungal hyphae. Xy - xylem vessels. Bar: 20 µm.

Figure 2. Activities of superoxide dismutase (SOD) (A), catalase (CAT) (B), ascorbate peroxidase (APX) (C), peroxidase (POX) (D), glutathione reductase (GR) (E), glutathione-S-transferase (GST) (F) and glutathione peroxidase (GPX) (E) determined in the leaves of maize plants non-inoculated (NI) or inoculated (I) with *Exserohilum turcicum*. For each evaluation time, means for the NI and I treatments followed by an asterisk (*) are significantly different based on *F*-test ($P \leq 0.05$). Bars represent the standard error of means.

Figure 3. Concentrations of hydrogen peroxide (H₂O₂) (A) and malondialdehyde (MDA) as well as electrolyte leakage (EL (%)) (C) in the leaves of maize plants non-inoculated (NI) or inoculated (I) with *Exserohilum turcicum*. For each evaluation time, means for the NI and I treatments followed by an asterisk (*) are significantly different based on *F*-test ($P \leq 0.05$). Bars represent the standard error of means.

Figure 4. Relative expressions of the genes superoxide dismutase (*sod*) (A), catalase (*cat*) (B), ascorbate peroxidase (*apx*) (C), peroxidase (*pox*) (D), glutathione reductase (*gr*) (E), glutathione-S-transferase and (*gst*) (F) on the leaves of maize plants inoculated with *Exserohilum turcicum*. Each evaluation time represents the average of four replicates. Bars represent the standard errors of means.

Table 1

Target genes ^a	Foward primer sequences (5' to 3')	Reverse primer sequences (3' to 5')
<i>sod</i>	TGTCACTGGAAGTGTCTCTG	CGCAGGATTGTAGTCGTGTC
<i>cat</i>	GATGGGTTGACGCACTGACA	AGATCCAAATGGTACGGTGTTC
<i>apx</i>	CTCAGGCAGGTTTTCTCCAC	AATCCAGACCTGTCCTTGTG
<i>pox</i>	AGCAGTGAGCTCAGTACACA	GCCGTTAGCTTGCTTTCCTT
<i>gr</i>	AAGCTGGATTGACGAAGCAA	TTTTCTAGTCGGGCTCCTCA
<i>gst</i>	GGCTAGTAATTCTGGAGCAGCTAGT	GCAAAAGTGCAACCAGTCCTTA
<i>gapdh</i>	AAGCCGGTCACCGTCTTT	CATCTTTGCTTGGGGCAGA

^aSuperoxide dismutase (*sod*), catalase (*cat*), ascorbate peroxidase (*apx*), peroxidase (*pox*), glutathione reductase (*gr*), glutathione-S-transferase (*gst*) and glyceraldehyde-3-phosphate dehydrogenase (*gapdh*).

Table 2

Variables	<i>F values</i> ^a		
	ST	PI	ST × PI
SOD	6.91 ^{**}	36.51 ^{**}	2.22 ^{ns}
CAT	2.99 [*]	10.43 ^{**}	0.46 ^{ns}
APX	6.01 [*]	76.12 ^{**}	7.04 ^{**}
POX	5.83 ^{**}	58.99 ^{**}	2.61 ^{ns}
GR	5.69 ^{**}	29.88 ^{**}	1.72 ^{ns}
GST	0.84 ^{ns}	14.49 ^{**}	1.77 ^{ns}
GPX	9.80 ^{**}	9.78 ^{**}	2.38 ^{ns}
H ₂ O ₂	2.21 ^{ns}	6.28 [*]	1.22 ^{ns}
MDA	1.61 ^{ns}	21.89 ^{**}	2.04 ^{ns}
EL(%)	4.85 ^{**}	61.62 ^{**}	8.47 ^{**}

Levels of probability: ^{ns} = non-significant, ^{*} = 0.05 and ^{**} = 0.01.

Table 3

Variables	Sev	SOD	CAT	APX	POX	GR	GST	GPX	H ₂ O ₂	MDA	EL
Sev	--	0.477*	0.253	0.600**	0.359	0.439*	-0.144	-0.366	0.293	0.018	0.525*
SOD		--	0.008	0.767**	0.685**	0.696**	0.093	0.018	0.169	-0.050	0.729**
CAT			--	-0.187	0.379	0.123	0.015	0.643**	0.328	-0.546*	0.131
APX				--	0.472*	0.511*	0.132	-0.331	-0.195	-0.007	0.768**
POX					--	0.506*	-0.254	0.401	0.134	-0.243	0.620**
GR						--	0.002	0.107	-0.125	-0.320	0.566**
GST							--	-0.358	-0.088	0.014	0.012
GPX								--	-0.083	0.311	0.114
H ₂ O ₂									--	0.164	0.280
MDA										--	0.262
EL											--

Levels of probability * = 0.05 and ** = 0.01.

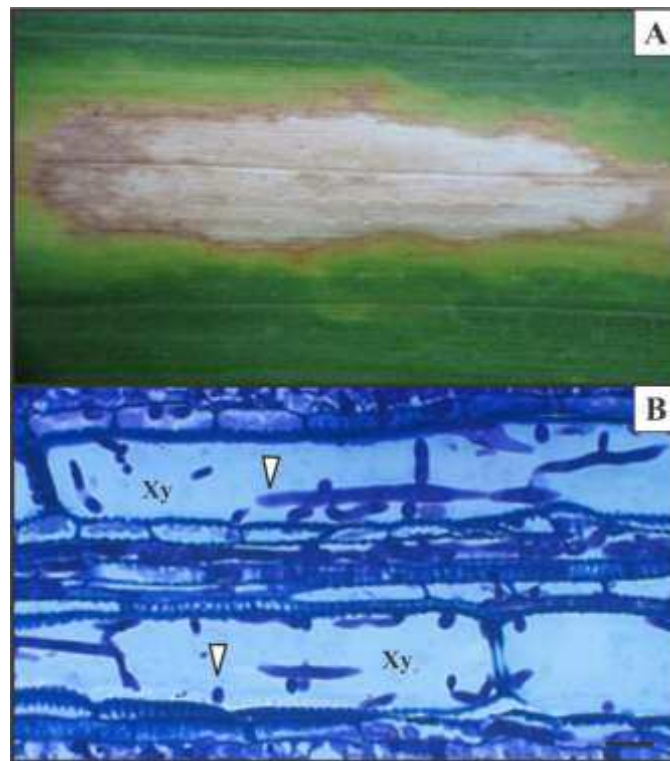


Figure 1

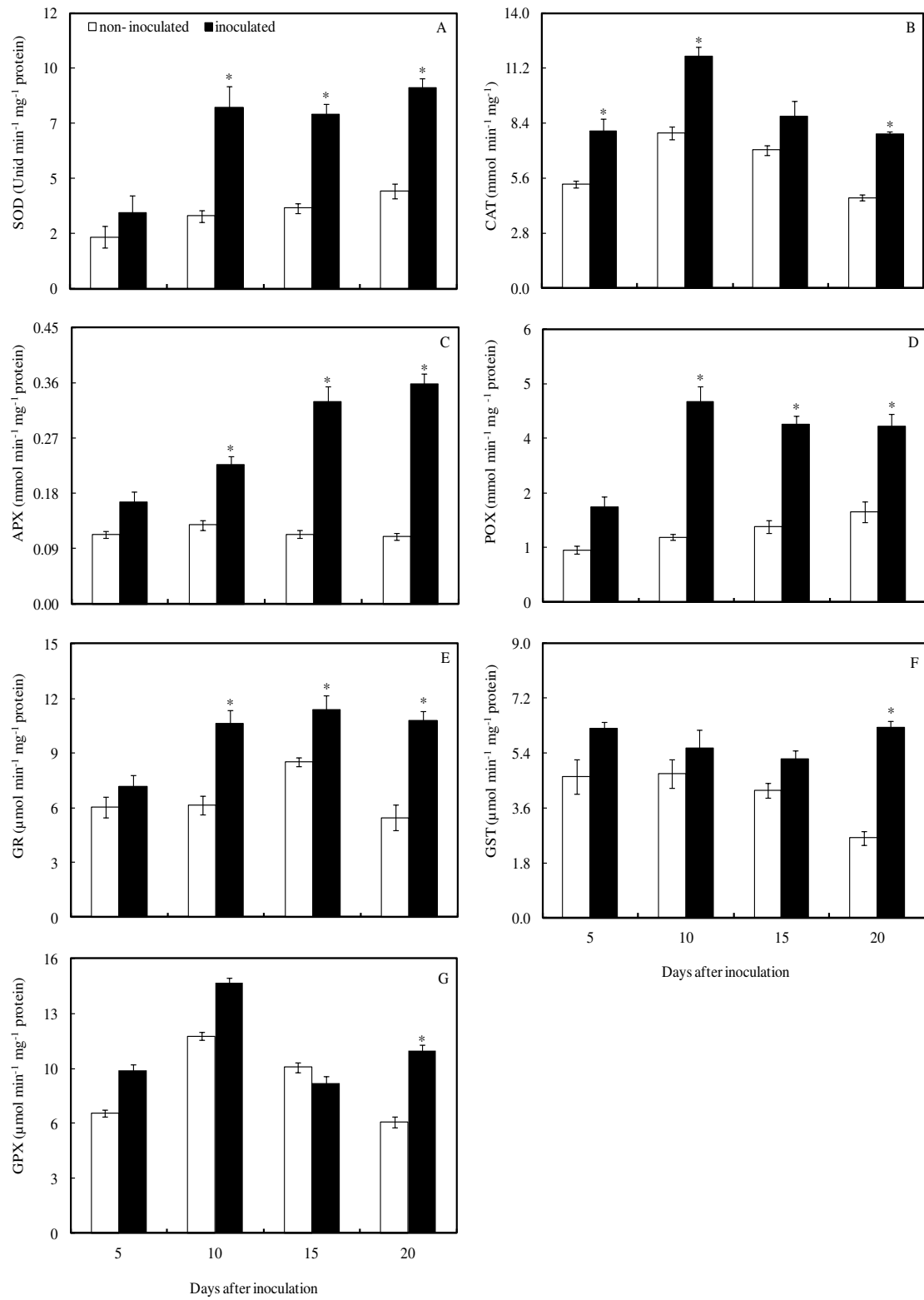


Figure 2

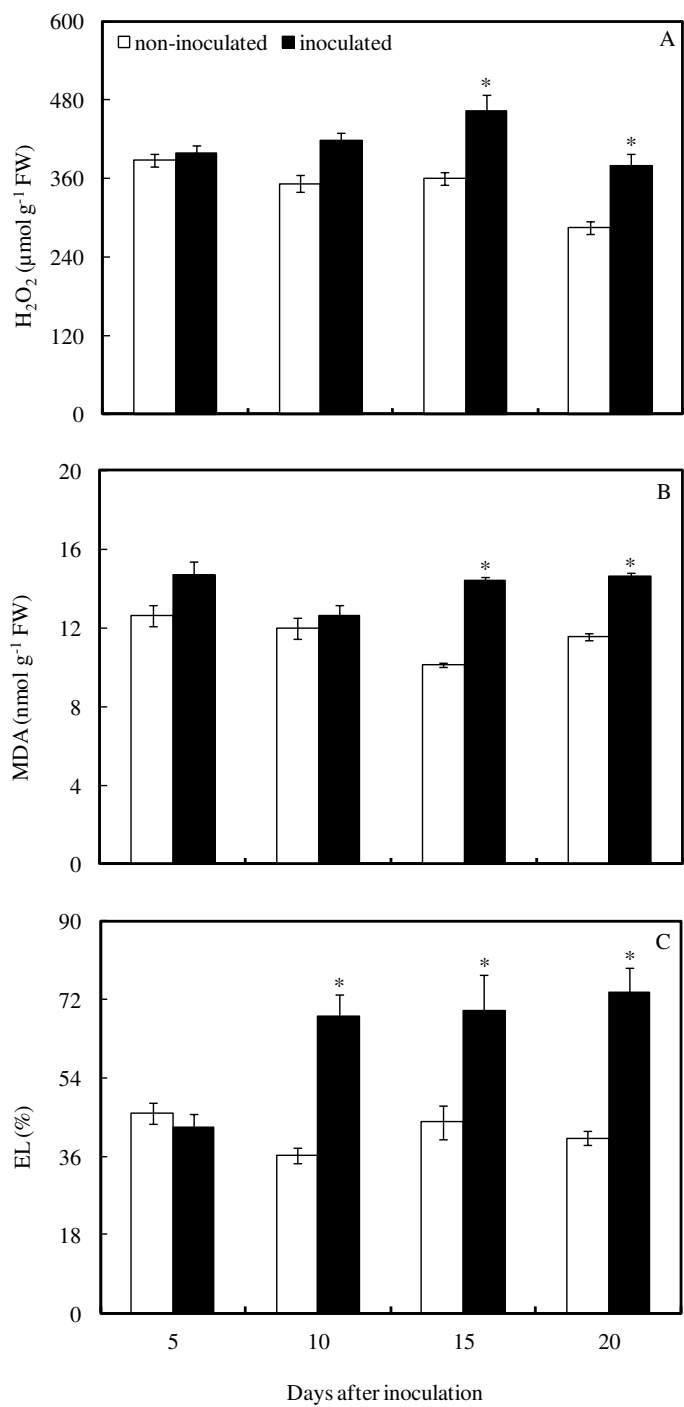


Figure 3

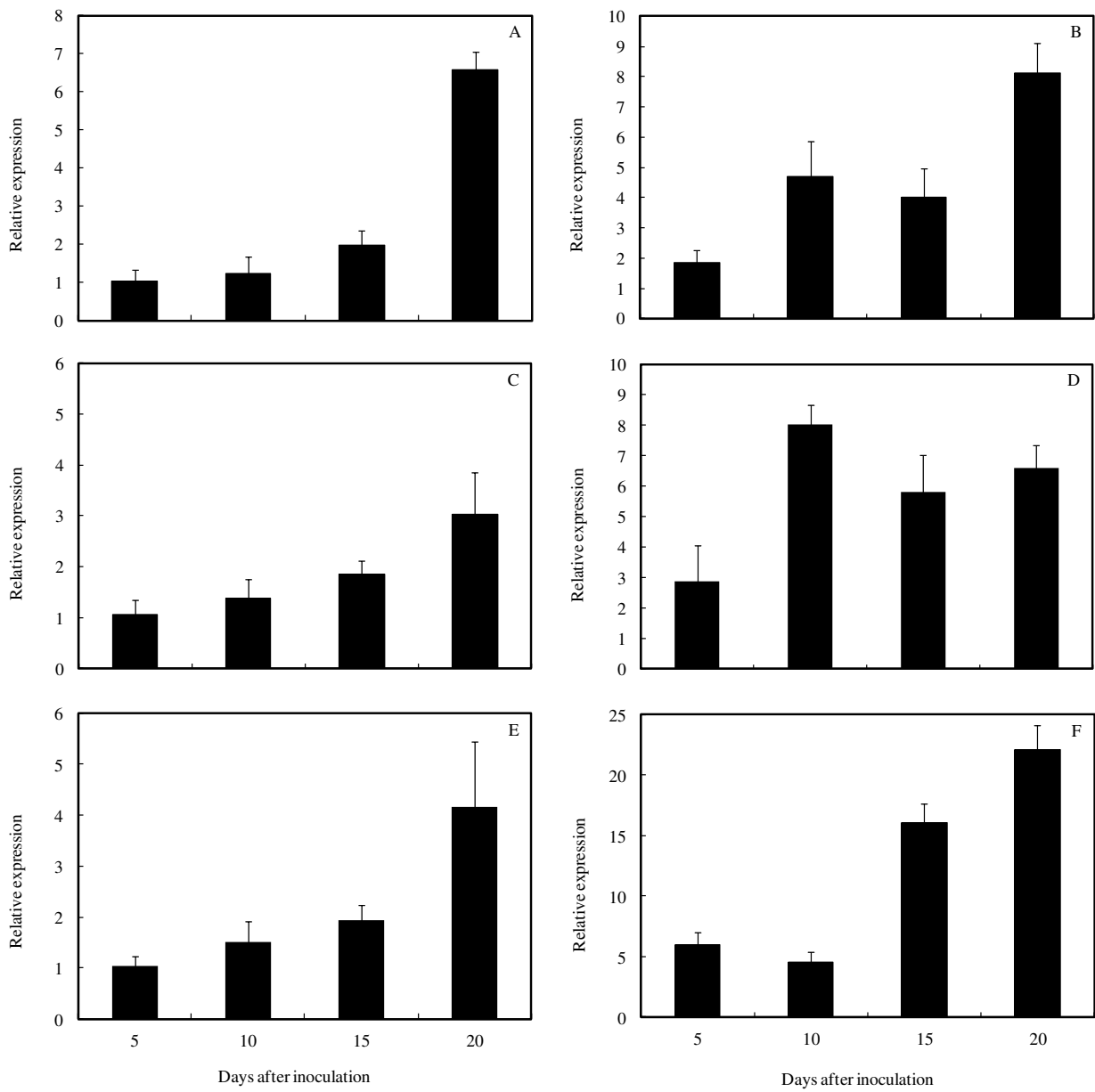


Figure 4

CHAPTER 2

Gas Exchange and Chlorophyll *a* Fluorescence on Maize Leaves Infected by *Exserohilum turcicum*

Abstract

This study aimed to investigate the photosynthetic changes in the leaves of maize plants infected by *Exserohilum turcicum*, which causes the northern leaf blight (NLB), an important disease occurring in all maize producing areas worldwide. The parameters related to leaf gas exchange (net carbon assimilation rate (A), stomatal conductance to water vapor (g_s), transpiration rate (E) and internal CO_2 concentration (C_i)) and of the chlorophyll (Chl) a fluorescence (maximum quantum yield of photosystem II (PSII) (F_v/F_m), effective quantum yield of photosystem II (PSII) ($Y(II)$), quantum yield of regulated energy dissipation ($Y(NPQ)$), quantum yield of non-regulated energy dissipation ($Y(NO)$) and electron transport rate (ETR)) were evaluated as well as the concentrations of photosynthetic pigments Chl_a , Chl_b and carotenoids. The values of A , g_s , E and C_i decreased as the symptoms of NLB developed. Changes in Chl a fluorescence parameters became evident at 10 days after inoculation (dai) and changes in the images began from 5 dai and intensified at advanced stages of fungal infection. The concentrations of Chl_a , Chl_b and carotenoids decreased in the leaves of infected plants at 15 and 20 dai. In conclusion, the results from the present study demonstrated, for the first time, that the photosynthesis on the leaves of maize plants was dramatically affected during the infection of process of *E. turcicum* mainly through limitations of diffusive and biochemical nature.

Introduction

Northern leaf blight (NLB), caused by the fungus *Exserohilum turcicum* (Pass.) Leonard and Suggs (anamorph) and *Setosphaeria turcica* (Luterell) Leonard and Suggs (teleomorph) (Leonard and Suggs, 1974; Luttrell and Bacon, 1977; Sivanesan, 1984), is a widespread disease in all producing maize areas worldwide and is capable to cause of significant yield mainly under conditions favorable for disease such as temperature between 18 and 27°C and high humidity (above 90%) (Adipala et al., 1993; CIMMYT, 2014). The yield losses can be greater than 50% when plants from susceptible cultivars are infected prior to flowering (Munkvold and White, 2016). The pathogen can survive in the soil or in the infected crop debris as mycelium and conidia are easily dispersed by rain splash and by the wind (Levy, 1984). The NLB symptoms in leaves are characterized by elliptical lesions with necrotic center and chlorotic halos and ranges from 2.5 to 15 cm and the lesions may coalesce giving the leaf an appearance of burning land dried (White, 1999). Plants when exposed to abiotic and biotic types of stresses their physiological processes changed mainly the photosynthesis, which is responsible for generating the basic resources necessary for plant maintenance (Berger et al., 2004; Berger et al., 2007; Bonfing et al., 2006). Photosynthesis starts with the absorption of light by the chlorophylls associated with the photosystem II (PSII), but this light energy can be lost as heat or fluorescence of chlorophyll or be directed to the photochemical phase of photosynthesis (Baker, 2008; Eberhard et al., 2008). This phase occurs through of the electron transport between the PSII and the photosystem I (PSI) that culminates in the formation of nicotinamide adenine dinucleotide phosphate (NADPH) and adenosine triphosphate (ATP), which are essential for a variety of metabolic processes in the plant, including CO₂ assimilation in the Calvin-Benson cycle and the synthesis of

photosynthetic pigments (Baker, 2008; Eberhard et al., 2008). The action of non-host selective toxins produced by the pathogens is also of pivotal importance to affect the photosynthesis due to the reduction in the concentration of chlorophylls (Chauhan et al., 1997). The stress caused by the pathogens infection can directly modify the photosynthetic process resulting, therefore, in significant changes in photosynthetic rates as well as the stomatal conductance, changes in the transpiration rates and also in the CO₂ concentration in the leaf tissue (Alves et al., 2011; Tatagiba et al., 2015; Bermúdez-Cardona et al., 2015a). The imaging of the Chlorophyll (Chl) *a* fluorescence has been used to better understand the photosynthetic changes in plants exposed to several types of stresses (Oxborough, 2004). It is a non-invasive, non-destructive and sensitive technique that provides a pre-symptomatic diagnosis of the disease before the visual symptoms appear and show changes in the photosynthetic apparatus of the stressed plants (Lichtenthaler and Miehe, 1997; Rolf and Scholes, 2010). Furthermore, the fluorescence image analysis of Chl *a* permits the study of the spatial-temporal heterogeneities in the fluorescence emission pattern within cells, leaves or even the whole plants (Gorbe and Calatayud, 2012). Inferences regarding the changes in photosynthesis can be verified by the parameters provided by fluorescence analysis of Chl *a* (Rolf and Scholes, 2010). Among these parameters, the maximum quantum efficiency of PSII (F_v/F_m) is one of the most common indicator of plant stress and its value in healthy plants is around 0.8 and decay as the leaf tissue become stresses. The parameter effective PSII quantum yield (Y(II)) is responsible for measuring the proportion of light which is absorbed by the chlorophylls used in the photochemical step in the photosynthesis (Baker, 2008; Maxwell and Johnson, 2000). The quantum yield of regulated energy dissipation (Y(NPQ)) and the quantum yield of energy dissipation non-regulated (Y(NO)) are other two important parameters used to verify the

functioning of the photosynthetic system of stressed (Bermúdez-Cardona et al., 2015b; Tatagiba et al., 2015). The Y(NPQ) reflects the down-regulation of the PSII which is a protective mechanism against the excess of light. Greater values of Y(NO) indicate that the photochemical energy conversion process as protection mechanisms is inefficient (Klughammer and Schreiber, 2008). Considering the importance of the NLB to reduce maize yield, this study aimed to determine the physiological changes occurring in plants infected with *E. turcicum* by analyzing their photosynthetic performance by combining the assessments of gas exchange associated with the fluorescence imaging of Chl *a* as well as the concentration of photosynthetic pigments.

Materials and Methods

Plant growth

Maize seeds from cultivar P-1630 Hx susceptible to *E. turcicum*, were sown in plastic pots containing 2 kg of Tropstrato[®] (Vida Verde, Mogi Mirim, São Paulo, Brazil) substrate composed of a 1:1:1 mixture of pine bark, peat and expanded vermiculite. A total of 1.63 g of calcium phosphate monobasic was added to each plastic pot. A total of three seeds were sown per pot and at five days after seedlings emergence, each pot was thinned to two seedlings. Plants were kept in a greenhouse during the experiments (temperature $25 \pm 3^\circ\text{C}$ during the day and $21 \pm 2^\circ\text{C}$ at night, relative humidity $75 \pm 5\%$) and were fertilized weekly with 50 mL of a nutrient solution composed of 192 mg L^{-1} KCl, 104.42 mg L^{-1} K_2SO_4 , 150.35 mg L^{-1} MgSO_4 , 61 mg L^{-1} $\text{CH}_4\text{N}_2\text{O}$, 0.27 mg L^{-1} $\text{NH}_4\text{MO}_7\text{O}_{24}$, 1.61 mg L^{-1} H_3BO_3 , 6.67 mg L^{-1} ZnSO_4 , 1.74 mg L^{-1} CuSO_4 , 4.10 mg L^{-1} MnCl_2 , 4.08 mg L^{-1} FeSO_4 and 5.58 mg L^{-1} ethylenediaminetetraacetic acid (EDTA).

The nutrient solution was prepared using deionized water. Plants were watered as needed.

Inoculum production and inoculation procedure

A monosporic isolate of *E. turcicum* ceded by the EPAGRI (Agricultural Research and Rural Extension Company of Santa Catarina) (UFV-DFP Et 17) was grown in Petri dishes containing lactose casein hydrolyzed medium (Malca and Ullstrup, 1962) kept in an incubator (25°C and photoperiod of 16 hours light and 8 hours dark) for ten days. Plants were inoculated with a conidial suspension of *E. turcicum* (1×10^4 conidia/ml) at 30 days after emergence (plants with five trifoliolate leaves fully expanded) (Bensch et al., 1992) using a VL a Airbrush atomizer (Paassche Airbrush Co, Chicago, IL). Gelatin (1% w/v) was added to the suspension to aid conidial adhesion to the leaf blades. At the 8th day after plants inoculation, a total of 200 leaf fragments ($\approx 0.25 \text{ cm}^2$) containing disease symptoms were collected, disinfected in a solution of 70% (v/v) aqueous alcohol and 2% sodium hypochlorite solution (v/v) and transferred to Petri dishes (five leaf fragments per Petri dish) containing lactose casein hydrolyzed medium. Petri dishes were then transferred to an incubator (25°C and photoperiod of 16 hours of light and 8 hours of dark) for ten days. After this period, a total of 1 ml of sterile distilled water was added to each Petri dish and fungal mycelia were carefully disrupted using camel-hair brush in a laminar flow chamber in order to induce fungal sporulation. After this procedure, Petri dishes were again transferred to an incubator (25°C and photoperiod of 12 h with black light lamps emitting light near the ultraviolet (320-400 nm) and 12 hours dark)) during five days. Plants with five trifoliolate leaves fully expanded were inoculated with a conidial suspension of *E. turcicum* as described above and then kept in a growth chamber (temperature of $25 \pm 2^\circ\text{C}$ and relative humidity of $90 \pm 5\%$) under

dark for the first 12 hours after inoculation in order to favor fungal infection. Thereafter, plants were transferred to a greenhouse (temperature of $25 \pm 2^\circ\text{C}$, relative humidity of $75 \pm 5\%$ and maximum natural photon flux density at plant canopy of $\approx 975 \mu\text{mol m}^{-2} \text{s}^{-1}$) for the duration of the experiments.

Assessment of NLB severity

Severity of NLB on the third fully expanded leaf, from the base to the top, for plants from each replication and treatment was evaluated at 8, 12, 16 and 20 days after inoculation (dai) using a set of standard area diagrams (Vieira et al., 2014).

Leaf gas exchange parameters

The leaf gas exchange parameters net carbon assimilation rate (A), stomatal conductance to water vapor (g_s), transpiration rate (E) and internal CO_2 concentration (C_i) were evaluated on the fourth leaf, from the base to top, of each plant per replication of each treatment at 5, 10, 15 and 20 dai using a portable open-flow gas ex (LI-6400XT, LI-COR, Lincoln, NE, USA). Evaluations were performed from 10:00 to 12:00 am under artificial light ($1200 \mu\text{mol photons m}^{-2} \text{s}^{-1}$) and CO_2 concentration of ± 400 ppm.

Determination of the concentration of photosynthetic pigments

Five leaf discs (8 mm in diameter) were collected from the third and fourth leaves, from the base to top, of each plant per replication of each treatment at 5, 10 15 and 20 dai. Leaf discs were also collected from non-inoculated plants at these same sampling times. Discs were transferred to glass vials containing 5 ml of dimethylsulfoxide (DMSO) (Santos et al., 2008). After 24 hours at 25°C , the absorbances of the extracts were read at 470, 649 and 665 nm using a DMSO as a blank (Wellburn et al., 1994).

Chlorophyll *a* fluorescence analysis

The images and fluorescence parameters of Chl *a* were obtained at 5, 10, 15 and 20 dai using a IMAGING-PAM fluorometer (Maxi version) and the Imaging Win software (Heinz Walz GmbH, Effeltrich, Germany). In order to obtain the images at a resolution of 640×480 pixels, the fourth leaf, from base to the top, of plant per replication of each treatment were individually fixed on a support at a distance of 18.5 cm from a charge coupled device (CCD) coupled to a fluorescence device. The leaf tissues were then exposed to a weak, modulated measuring beam ($0.5 \mu\text{mol m}^{-2} \text{s}^{-1}$, 100 μs , 1 Hz) to determine the initial fluorescence (F_0). Next, a saturating white light pulse of $2.400 \mu\text{mol m}^{-2} \text{s}^{-1}$ (10 Hz) was applied for 0.8 s to ensure the maximum fluorescence emission (F_m). From these initial measurements, the maximum PS II photochemical efficiency of the dark-adapted leaves was estimated through the variable to maximum Chl *a* fluorescence ratio, $F_v/F_m = [(F_m - F_0)/F_m]$. The leaf tissues were subsequently exposed to actinic photon irradiance ($80 \mu\text{mol m}^{-2} \text{s}^{-1}$) for 180 s to obtain the steady-state fluorescence yield (F_s), after which a saturating white light pulse ($2400 \mu\text{mol m}^{-2} \text{s}^{-1}$; 0.8 s) was applied to achieve the light-adapted maximum fluorescence (F_m'). The light-adapted initial fluorescence (F_0') was estimated according to Oxborough and Baker (1997). Following the calculations of Kramer et al. (2004), the effective PSII quantum yield [$Y(\text{II}) = (F_m' - F_s)/F_m'$], the quantum yield of regulated energy dissipation [$Y(\text{NPQ}) = (F_s/F_m') - (F_s/F_m)$], the quantum yield of non-regulated energy dissipation [$Y(\text{NO}) = F_s/F_m$] and electron transport rate (ETR) were calculated ($\Phi\text{PSII} \cdot \text{PPFD} \cdot f \cdot \alpha$).

Experimental design and statistical analysis

Two experiments (Experiments 1 and 2), consisting of two treatments (non-inoculated and inoculated plants), was arranged in a completely randomized design with four replications to evaluate disease severity as well as the leaf gas exchange parameters. Two other experiments (Experiments 3 and 4) were performed to obtain the Chl *a* fluorescence parameters and consisted of two treatments (non-inoculated and inoculated plants) and arranged in a completely randomized design with four replications. Each experimental unit corresponded to a plastic pot containing two plants. Data from NLB severity and leaf gas exchange parameters from Experiments 1 and 2 and from the Chl *a* fluorescence parameters from Experiments 3 and 4 were analyzed using the MIXED procedure of the SAS software (Release 8.02 Level 02M0 for Windows, SAS Institute, Inc., 1989, Cary, NC, USA) to determine if data from these experiments could be combined (Moore and Dixon, 2015). For all variables evaluated, the ANOVA was considered 2×4 factorial experiment consisting of non-inoculated and inoculated plants (plant inoculation (PI)) and four sampling time (ST). Data from all variables were analyzed by ANOVA and means from the treatments were compared with the *F*-test using SAS (version 6.12; SAS Institute, Inc., Cary, NC). Data from each parameter were correlated among them using Pearson correlation.

Results

Disease severity

Disease severity increased by 1.6, 5, 15 and 37% at 8, 12, 16 and 20 dai, respectively, on the leaves of maize plants (Fig. 1)

Leaf gas exchange parameters

The factors PI and ST were significant for all parameters evaluated and the interaction PI \times ST was significant only for A and g_s (Table 1). There were significant decreases of 13, 20, 40 and 59% for A , of 33, 45, 55 and 87% for g_s , of 34, 41, 33 and 52% for E and of 7, 10, 6 and 12% for C_i , respectively, at 5, 10, 15 and 20 dai for inoculated plants in comparison to the non-inoculated ones (Fig. 2A-D).

Concentration of photosynthetic pigments

The factors PI and ST as well as the interaction PI \times ST were significant for the concentrations of Chl_a , Chl_b and carotenoids (Table 1). There were significant decreases of 52 and 58% for the concentration of Chl_a , of 51 and 58% for the concentration of Chl_b and of 34 and 51% for the concentration of carotenoids at 15 and 20 dai, respectively, for inoculated in comparison to the non-inoculated ones (Fig. 3A-C).

Chlorophyll a fluorescence parameters

The factors PI and ST as well as the interaction PI \times ST were significant for F_v/F_m , $Y(II)$, NPQ, $Y(NO)$ and ETR (Table 1). For inoculated plants, the values for F_v/F_m were significantly reduced by 4% at 10 dai, 4% at 15 dai and by 12% at 20 dai in comparison to the non-inoculated ones (Fig 4A). The values for $Y(II)$ were significantly reduced by 18 and 25% at 15 and 20 dai, respectively, for inoculated plants in comparison to the non-inoculated ones (Fig. 4B). The values for $Y(NPQ)$ significantly increased by 22 and 24% at 10 and 15 dai, respectively and decreased by 8% at 20 dai for inoculated plants in comparison to the non-inoculated ones (Fig. 3C). The values for $Y(NO)$ significantly increased by 18 and 37%, respectively, at 15 and 20 dai for

inoculated plants in comparison to the non-inoculated ones (Fig. 4D). The values for ETR were significantly lower by 12, 19 and 35%, respectively, at 10, 15 and 20 dai for inoculated plants in comparison to the non-inoculated ones (Fig. 4E). Changes in the images of the Chl *a* fluorescence were first noticed at 5 dai and became more evident at 15 and 20 dai as indicated by the dark areas that corresponded to the necrotic lesions. In the necrotic lesions, there were decreases in the values of F_v/F_m and Y(II) and increases in the values of NPQ at 10 and 15 dai following by increase in the values of Y(NO) at 15 and 20 dai (Fig. 5).

Pearson correlation

The four leaf gas exchange parameters, chlorophyll *a* fluorescence parameters (with exception of Y(NO)) and the concentrations of Chl_{*a*}, Chl_{*b*} and carotenoids were negatively correlated with disease severity. The four leaf gas exchange parameters were positively correlated with each other, with the concentrations of Chl_{*a*}, Chl_{*b*} and carotenoids and with the chlorophyll *a* fluorescence parameters F_v/F_m , Y(II) and ETR, but negatively correlated with Y(NO). Y(NPQ) was negatively correlated with *A*, *g_s* and *C_i* and positively correlated with *E*. F_v/F_m was positively correlated with Y(II), ETR and with the concentrations of Chl_{*a*}, Chl_{*b*} and carotenoids and negatively correlated with Y(NPQ) and Y(NO). Y(II) was positively correlated with ETR and with the concentrations of Chl_{*a*}, Chl_{*b*} and carotenoids and negatively correlated with Y(NPQ) and Y(NO). Y(NPQ) was negatively correlated with Y(NO) and ETR as well as with the concentrations of Chl_{*a*}, Chl_{*b*} and carotenoids. The concentrations of Chl_{*a*}, Chl_{*b*} and carotenoids were positively correlated with each other as well as with ETR (Table 2).

Discussion

This study provides novel information regarding the alterations of the photosynthesis on the leaves of maize plants during the infection process of *E. turcicum*. The values of the leaf gas exchange parameters decreased on the infected leaves in comparison to the non-infected ones even before the appearance of disease symptoms that only occurred after 8 dai. In relation to the parameters of Chl *a* fluorescence, most of them began to be significantly altered in the infected leaves at 10 dai although the changes in the images of these parameters occurred from 5 dai in comparison to the images obtained from the non-infected leaves. This fact confirms the use of the Chl *a* fluorescence imaging as a useful tool provide information regarding the changes in the physiological processes related to the photosynthetic performance of plants before the occurrence of the incubation period of the disease (Lichtenthaler and Miede 1997; Chaerle et al., 2004; Mutka and Bart, 2015). Regarding the analysis of the leaf gas exchange parameters, several studies reported a decrease in *A* associated with low and high values for g_s and C_i , respectively (Lopes and Berger, 2001; Tatagiba et al., 2015; Bermúdez-Cardona et al., 2015a). In this case, the photosynthetic restrictions can be attributed to limitation on CO_2 fixation at the biochemical level and not due to reduced CO_2 influx due to stomatal closure as reported by Alves et al. (2011) and Debona et al. (2014). However, in the present study the reverse was observed for the infected leaves. The reductions in *A* appeared to be related to stomatal limitations since it was accompanied by decreases in the values of both g_s and C_i indicating, therefore, a smaller influx of CO_2 into the leaf tissues that consequently may have contributed to the restriction on the photosynthetic rate of the infected leaves. Similar results were observed for mango plants infected by *Ceratocystis fimbriata* which showed less CO_2 influx that was accompanied by

reductions in both internal and ambient CO₂ concentration ratio (Bispo et al., 2016). Dallagnol et al. (2015) reported reductions in A associated with significant decreases in both g_s and C_i in rice plants infected by *Bipolaris oryzae*. The authors attributed the reduction in CO₂ influx to changes in stomatal opening induced by the non-host selective toxins produced by *B. oryzae*. In the present study, the reductions in A were accompanied by lower values of both g_s and C_i that could be confirmed by the positive and significant correlation among these parameters. The decrease in E on the maize leaves infected by *E. turcicum* can be attributed to stomatal closure and corroborates with the findings obtained for the maize-*Stenocarpella macrospora* interaction (Bermúdez-Cardona et al., 2015a). According to Bermúdez-Cardona et al. (2015a), the dried leaves, as a result of disease development, contributed to stomatal closure in order to avoid the excessive loss of water and thereby leading to reductions in E . This can also be the case for the maize-*E. turcicum* interaction, since a common feature of the disease symptom is the drying of the leaves, specially at the advanced stages of disease development where there was drastic decreased on the E values. Photosynthetic pigments, especially the chlorophylls, are intrinsically linked to photosynthesis since they are responsible for light absorption and the subsequent transference of energy to the reaction centers where occurs the photochemical phase of the photosynthesis (Taiz and Zeiger, 2009). In the present study, decrease of more than 50% in the concentrations of Chl_a, Chl_b and carotenoids occurred from 15 to 20 dai for the infected leaves in comparison to the non-infected ones. It is known that *E. turcicum* produces the Ht-toxin that besides causing damage to the cell membranes can also inhibits the synthesis of chlorophylls in maize cultivars susceptible to NLB (Bashan and Levy, 1992; Chauhan et al., 1997). Thus, the production of Ht-toxin by *E. turcicum* may have helped in reducing the concentration of photosynthetic pigments contributing, therefore,

to reduction in the A values, especially at advanced stages of fungal infection. The Chl a fluorescence image has allowed noticing the changes in photosynthesis on the plants infected during the infection process of the pathogens with different life styles (Scholes and Rolf, 2009). Analysis of Chl a fluorescence image of wheat leaves infected with *Mycosphaerella graminicola*, a hemibiotrophic fungus, showed no change in the values of F_v/F_m , $Y(II)$ and NPQ during its biotrophic phase indicating, therefore, that the fungus did not cause any damage to the photosynthetic apparatus or even influenced the photosynthetic capacity of the infected plants in comparison to the non-infected ones. During the necrotrophic phase of *E. turcicum*, especially at 17 dai, significant decreases on the values of F_v/F_m , $Y(II)$ and NPQ were observed indicating, therefore, damage to the photosynthetic apparatus and photosynthetic changes (Scholes and Rolf, 2009). In the present study, the evaluation of the Chl a fluorescence parameters at 5 dai on the leaves of inoculated plants did not show any changes in comparison to the leaves of non-infected plants although small changes in the images were noticed, but not as the drastic changes that occurred at advanced stages of fungal infection. This finding indicates that at early stage of fungal infection, it was able to cause direct damage to the photosynthetic apparatus. Thus, the significant reduction in A observed at 5 dai can possibly be explained by the low capacity of the leaves to keep greater CO_2 concentration due to stomatal restrictions. At the beginning of the disease symptoms 8 dai, reductions in the values of F_v/F_m were noticed. This parameter represents the maximum quantum yield of PSII when the reaction centers are open (oxidized) (Baker, 2008). Reductions in the values of $Y(II)$ were more pronounced at advanced stages of *E. turcicum* infection and, consequently, when the disease symptoms became more evident. The $Y(II)$ measures the proportion of light absorbed by the chlorophylls associated with the PSII which is actually used in the photochemical step in the

photosynthesis (Maxwell and Johnson, 2000). Reductions on Y(II) occur due to pathogens infection and are associated with damage to the photosynthetic apparatus (Meyer et al., 2001). Parallel to decreases in the values of both F_v/F_m and Y(II), reduction in ETR was also noticed indicating, therefore, that the electron transport was also impaired due to damage in the photosynthetic apparatus. The ETR is a good indicator of the overall functioning of photosynthesis (Maxwell and Johnson, 2000). Thus, the reduction in the values of this parameters are associated with changes in the other parameters confirming, therefore, the damage caused by *E. turcicum* on the photosynthesis. It is known that one alternative to protect the photosynthetic apparatus is the release of heat through the non-photochemical fluorescence quenching represented by Y(NPQ) which contributes to the regulation of energy involved in the photosynthetic (Maxwell and Johnson, 2000; Klughammer and Schreiber, 2008). When the efficiency of the photochemical processes increases, it leads to decrease in the quantum yield of the non-photochemical process and vice versa (Roháček et al., 2008). In general, plants under stress show an increase in the values of Y(NPQ) indicating, therefore, an inefficiency of the photochemical process that is reflected in the increased release of energy as heat. In the present study, a significant increase in the values of Y(NPQ) was observed from 10 to 15 dai for infected leaves in comparison to non-infected ones indicating, therefore, a reduction in the photochemical efficiency. At advanced stages of fungal infection, decreases in the values of Y(NPQ) were accompanied by increases in the values of Y(NO). High values of Y(NO) indicated that both photochemical energy conversion and protective regulatory mechanisms became inefficient (Klughammer and Schreiber, 2008). Maize leaves infected with *S. macrospora* also showed decreases in the values of Y(NPQ) that were accompanied by increase in the values of Y(NO) at advanced stages of fungal infection (Bermúdez-

Cardona et al., 2015b). In conclusion, the results from the present study demonstrated, for the first time, that photosynthesis in the leaves of maize plants was dramatically affected during the infection of process of *E. turcicum* mainly through limitations of diffusive and biochemical nature.

References

- Adipala E, Lipps PE, Madden LV, 1993. Reaction of maize cultivars from Uganda to *Exserohilum turcicum*. *Phytopathology* 83, 217-23.
- Alves AL, Guimarães AGMC, DaMatta FM, Alfenas AC, 2011. Leaf gas exchange and chlorophyll *a* fluorescence of *Eucalyptus urophylla* in response to *Puccinia psidii* infection. *Acta Physiologiae Plantarum* 33, 1831-39.
- Baker NR, 2008. Chlorophyll Fluorescence: a probe of photosynthesis *in vivo*. *Annual Review of Plant Biology* 59, 89-113.
- Bashan B, Levy Y, 1992. Differential response of sweet corn cultivars to phytotoxic water-soluble compounds from culture filtrates of *Exserohilum turcicum*. *Plant Disease* 76, 451-54.
- Bensch MJ, Van staden J, Rijkenberg JHF, 1992. Time and site of inoculation of maize for optimum infection of ears by *Stenocarpella maydis*. *Journal of Phytopathology* 136 265-69.
- Bermúdez-Cardona MB, Wordell Filho JA, Rodrigues FA, 2015a. Leaf gas exchange and chlorophyll *a* fluorescence in maize leaves infected with *Stenocarpella macrospora*. *Phytopathology* 105, 26-34.
- Bermúdez-Cardona MB, Bispo WMS, Rodrigues FA, 2015b. Physiological and biochemical alterations on maize leaves infected by *Stenocarpella macrospora*. *Acta Physiologiae Plantarum* 37, 1-17.
- Bispo WMS, Araujo L, Moreira WR, Silva LC, Rodrigues FA, 2016. Differential leaf gas exchange performance of mango cultivars infected by different isolates of *Ceratocystis fimbriata*. *Scientia Agricola* 73, 150-58.

Berger S, Papadopoulos M, Schreiber U, Kaiser W, Roitsch T, 2004. Complex regulation of gene expression, photosynthesis and sugar levels by pathogen infection in tomato. *Physiologia Plantarum* 122, 419-28.

Berger S, Sinha AK, Roitsch T, 2007. Plant physiology meets phytopathology: plant primary metabolism and plant-pathogen interactions. *Journal of Experimental Botany* 58, 4019-26.

Bonfing KB, Schreiber U, Gabler A, Roitsch T, Berger S, 2006. Infection with virulent and avirulent *P. syringae* strain differentially affects photosynthesis and sink metabolism in *Arabidopsis* leaves. *Planta* 225, 1-12.

Chaerle L, Hagenbeek D, De Bruyne E, Valcke R, Van Der Straeten D, 2004. Thermal and chlorophyll-fluorescence imaging distinguish plant-pathogen interactions at an early stage. *Plant Cell Physiology* 45, 887-96.

Chauhan RS, Singh BM, Develash RK, 1997. Effect of toxic compounds of *Exserohilum turcicum* on chlorophyll content, callus growth and cell viability of susceptible and resistant inbred lines of maize. *Journal of Phytopathology* 145, 435-40.

CIMMYT, 2014. Maize Annual Report: Research Program on Maize. GGIAR. 48 p.

Dallagnol LJ, Martins SCV, DaMatta FM, 2015. Brown spot negatively affects gas exchange and chlorophyll *a* fluorescence in rice leaves. *Tropical Plant Pathology* 40, 275-78.

Debona D, Rodrigues FA, Rios JA, Martins SCV, Pereira LF, DaMatta FM, 2014. Limitations to photosynthesis in leaves of wheat plants infected by *Pyricularia oryzae*. *Phytopathology* 104, 34-39.

Eberhard S, Finazzi G, Wollman FA, 2008. The dynamics of photosynthesis. *Annual Review of Genetic* 42, 463-515.

- Gorbe E, Calatayud A, 2012. Applications of chlorophyll fluorescence imaging technique in horticultural research: a review. *Scientia Horticulturae* 138, 24-35.
- Klughammer C, Schreiber U, 2008. Complementary PSII quantum yields calculated from simple fluorescence parameters measured by PAM fluorometry and the saturation pulse method. *PAM Application Notes* 1, 27-35.
- Kramer DM, Johnson G, Kiirats O, Edwards GE, 2004. New fluorescence parameters for the determination of Q_A redox state and excitation energy fluxes. *Photosynthesis Research* 79, 209-18.
- Leonard KJ, Suggs EG, 1974. *Setosphaeria prolata* the ascigerous state of *Exserohilum prolatum*. *Mycologia* 66, 281-97.
- Levy Y, 1984. Overwintering of *Exserohilum turcicum* in Israel. *Phytoparasitica* 12, 177-82.
- Lichtenthaler HK, Miehe JA, 1997. Fluorescence imaging as a diagnostic tool for plant stress. *Trends in Plant Science* 2, 316-20.
- Lopes DB, Berger RD, 2001. The effects of rust and anthracnose on the photosynthetic competence of diseased bean leaves. *Phytopathology* 91, 212-20.
- Luttrell ES, Bacon CW, 1977. Classification of *Myriogenospora* in the Clavicipitaceae. *Canadian Journal Botany* 55, 20900-97.
- Malca I, Ullstrup AJ, 1962. Effects of carbon and nitrogen nutrition on growth and sporulation of two species of *Helminthosporium*. *Bulletin Torrey Botanical Club* 89, 240-49.
- Maxwell K, Johnson GN, 2000. Chlorophyll fluorescence-a practical guide. *Journal of Experimental Botany* 5, 659-68.

- Meyer S, Saccardy-Adji K, Rizza F, Genty B, 2001. Inhibition of photosynthesis by *Colletotrichum lindemuthianum* in bean leaves determined by chlorophyll fluorescence imaging. *Plant Cell Environmental* 24, 947-55.
- Moore KJ, Dixon P, 2015. Analysis of Combined Experiments Revisited. *Agronomy Journal* 107, 763-71.
- Mutka AM, Bart RS, 2015. Image-based phenotyping of plant disease symptoms. *Frontiers in Plant Science* 5, 1-8.
- Oxborough K, Baker NR, 1997. Resolving chlorophyll a fluorescence images of photosynthetic efficiency in to photochemical and non photochemical components - calculation of qP and F_v'/F_m' without measuring F_0' . *Photosynthesis Research* 54, 135-42.
- Oxborough K, 2004. Imaging of chlorophyll a fluorescence: theoretical and practical aspects of an emerging technique for the monitoring of photosynthetic performance. *Journal of Experimental Botany* 55, 1195-1205.
- Roháček K, Soukupová J, Barták M, 2008. Chlorophyll fluorescence: a wonderful tool to study plant physiology and plant stress. *Plant Cell Compartments - Selected Topics* 37, 41-104.
- Rolf SA, Scholes JD, 2010. Chlorophyll fluorescence imaging of plant-pathogen interactions. *Protoplasma* 247, 163-75.
- Santos RP, Cruz ACF, Iarema L, Kuki KN, Otoni WC, 2008. Protocolo para extração de pigmentos foliares em porta-enxertos de videira micropropagados. *Ceres* 55, 356-64.
- Scholes JD, Rolfe SA, 2009. Chlorophyll fluorescence imaging as tool for understanding the impact of fungal diseases on plant performance: a phenomics perspective. *Functional Plant Biology* 36, 880-92.

- Sivanesan A, 1984. The bitunicate ascomycetes and their anamorphs. *Canadian Journal of Botany* 67, 1500-99.
- Tatagiba SD, DaMatta FM, Rodrigues FA, 2015. Leaf gas exchange and chlorophyll *a* fluorescence imaging of rice leaves infected with *Monographella albescens*. *Phytopathology* 105, 180-88.
- Taiz L, Zeiger E, 2009. Fisiologia Vegetal, 4^a Ed, Artmed, Porto Alegre.
- Vieira RA, Mesquini RM, Silva CN, Hata FT, Tessmann DJ, Scapim CA, 2014. A new diagrammatic scale for the assessment of northern corn leaf blight. *Crop Protection* 56, 55-7.
- Wellburn AR, 1994. The spectral determination of chlorophylls *a* and *b*, as well as total carotenoids, using various solvents with spectrophotometers of different resolution. *Journal of Plant Physiology* 144, 307-13.
- White DG, Munkvold GP. Compendium of corn diseases. 4rd Ed. St. Paul, MN, USA: The American Phytopathological Society.

List of Tables and Figures

Table 1. Analysis of variance of the effects of plant inoculation (PI) and sampling time (ST) as well as their interactions (PI \times ST) on net CO₂ assimilation rate (A), stomatal conductance to water vapor (g_s), transpiration rate (E), internal CO₂ concentration (C_i), maximum quantum yield of photosystem II (PSII) (F_v/F_m), effective quantum yield of photosystem II (PSII) $Y(II)$, quantum yield of regulated energy dissipation $Y(NPQ)$, quantum yield of non-regulated energy dissipation $Y(NO)$, electron transport rate (ETR) as well as on the concentrations of chlorophyll a (Chl_a), Chl_b and carotenoids (Car).

Table 2. Pearson correlation coefficients among disease severity (Sev), net CO₂ assimilation rate (A), stomatal conductance to water vapor (g_s), transpiration rate (E), internal CO₂ concentration (C_i), maximum quantum yield of photosystem II (PSII) (F_v/F_m), effective quantum yield of photosystem II (PSII) $Y(II)$, quantum yield of regulated energy dissipation $Y(NPQ)$, quantum yield of non-regulated energy dissipation $Y(NO)$, electron transport rate (ETR) as well as concentrations of chlorophyll a (Chl_a), Chl_b and carotenoids (Car) in the leaves maize plants inoculated with *Exserohilum turcicum*.

Figure 1. Severity of northern leaf blight on the leaves of maize of maize plants. Bars represent the standard error of the means $n = 4$.

Figure 2. Net CO₂ assimilation rate (A) (A), stomatal conductance to water vapor (g_s) (B), transpiration rate (E) (C) and internal CO₂ concentration (C_i) (D) determined in the leaves of maize plants non-inoculated (NI) or inoculated (I) with *Exserohilum turcicum*. For each evaluation time, means for the NI and I treatments that are followed by an

asterisk (*) are significantly different based on the F -values ($P \leq 0.05$). Bars represent the standard error of the means.

Figure 3. Concentrations of chlorophyll a (Chl $_a$) (A), Chl $_b$ (B) and carotenoids (C) in the leaves of maize plants non-inoculated (NI) or inoculated (I) with *Exserohilum turcicum*. For each evaluation time, means for the NI and I treatments that are followed by an asterisk (*) are significantly different based on the F -values ($P \leq 0.05$). Bars represent the standard error of the means.

Figure 4. Maximum quantum yield of photosystem II (PSII) (F_v/F_m) (A), effective quantum yield of photosystem II (PSII) Y(II) (B), quantum yield of regulated energy dissipation Y(NPQ) (C), quantum yield of non-regulated energy dissipation Y(NO) (D) and electron transport rate (ETR) (E) determined in the leaves of maize plants non-inoculated (NI) or inoculated (I) with *Exserohilum turcicum*. For each evaluation time, means for the NI and I treatments that are followed by an asterisk (*) are significantly different based on the F -values ($P \leq 0.05$). Bars represent the standard error of the means.

Figure 5. Images of chlorophyll a fluorescence parameters: the maximum quantum yield of photosystem II (F_v/F_m), the effective quantum yield of photosystem II Y(II), the quantum yield of regulated energy dissipation Y(NPQ) and the quantum yield of non-regulated energy dissipation Y(NO) measured in the leaves of maize plants non-inoculated (NI) or inoculated (I) with *Exserohilum turcicum* at 5, 10, 15 and 20 days after inoculation (dai).

Table 1

Variables	<i>F</i> - values ^a		
	ST	PI	ST × PI
<i>A</i>	100**	849.23**	79.23**
<i>g_s</i>	71.05**	411.82**	10.59**
<i>E</i>	11.19**	197.54**	24.29 ^{ns}
<i>C_i</i>	101.83**	44.88**	54.29 ^{ns}
<i>F_v/F_m</i>	3.9**	56.90**	18.19**
<i>Y(II)</i>	21.79**	28.80**	5.79*
<i>Y(NPQ)</i>	14.15**	27.42**	5.99**
<i>Y(NO)</i>	22.40**	57.99**	29.13**
<i>ETR</i>	36.55**	64.93**	9.69**
<i>Chl_a</i>	15.7**	51.81**	13.64**
<i>Chl_b</i>	23.60**	31.54**	16.42**
<i>Car</i>	13.37**	50.56**	8.83**

Levels of probability: ^{ns} = non-significant,
* = 0.05 and ** = 0.01.

Table 2

Variables	Sev	A	g_s	E	C_i	F_v/F_m	Y(II)	Y(NPQ)	Y(NO)	ETR	Chl _a	Chl _b	Car
Sev	--	-0.908**	-0.863**	-0.595**	-0.839**	-0.859**	-0.904**	-0.027	0.856**	-0.772**	-0.806**	-0.830**	-0.715*
A		--	0.985**	0.686*	0.839**	0.831**	0.901**	-0.090	-0.925**	0.786**	0.894**	0.892**	0.731*
g_s			--	0.755*	0.971**	0.981**	0.929**	-0.146	-0.758**	0.810**	0.756*	0.764**	0.629*
E				--	0.743*	0.610*	0.608*	0.332	-0.696*	0.561*	0.504*	0.382*	0.703*
C_i					--	0.910**	0.913**	-0.122	-0.700*	0.725*	0.673*	0.708*	0.621*
F_v/F_m						--	0.855**	-0.172	-0.718*	0.794*	0.653*	0.736*	0.571*
Y(II)							--	-0.258	-0.769**	0.742*	0.850**	0.892**	0.663*
Y(NPQ)								--	-0.149	-0.041	-0.179	-0.302	-0.351
Y(NO)									--	-0.729*	-0.809**	-0.790**	-0.759**
ETR										--	0.713*	0.712*	0.632*
Chl _a											--	0.927**	0.779**
Chl _b												--	0.657*
Car													--

Levels of probability: * = 0.05 and ** = 0.01.

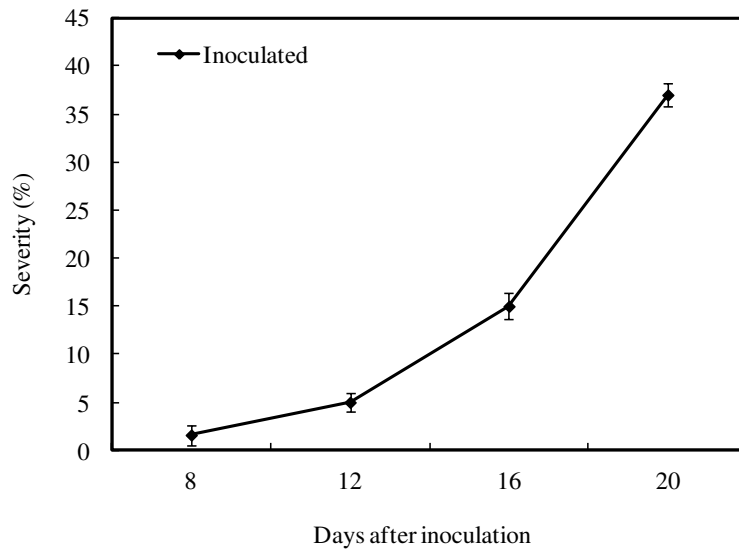


Figure 1

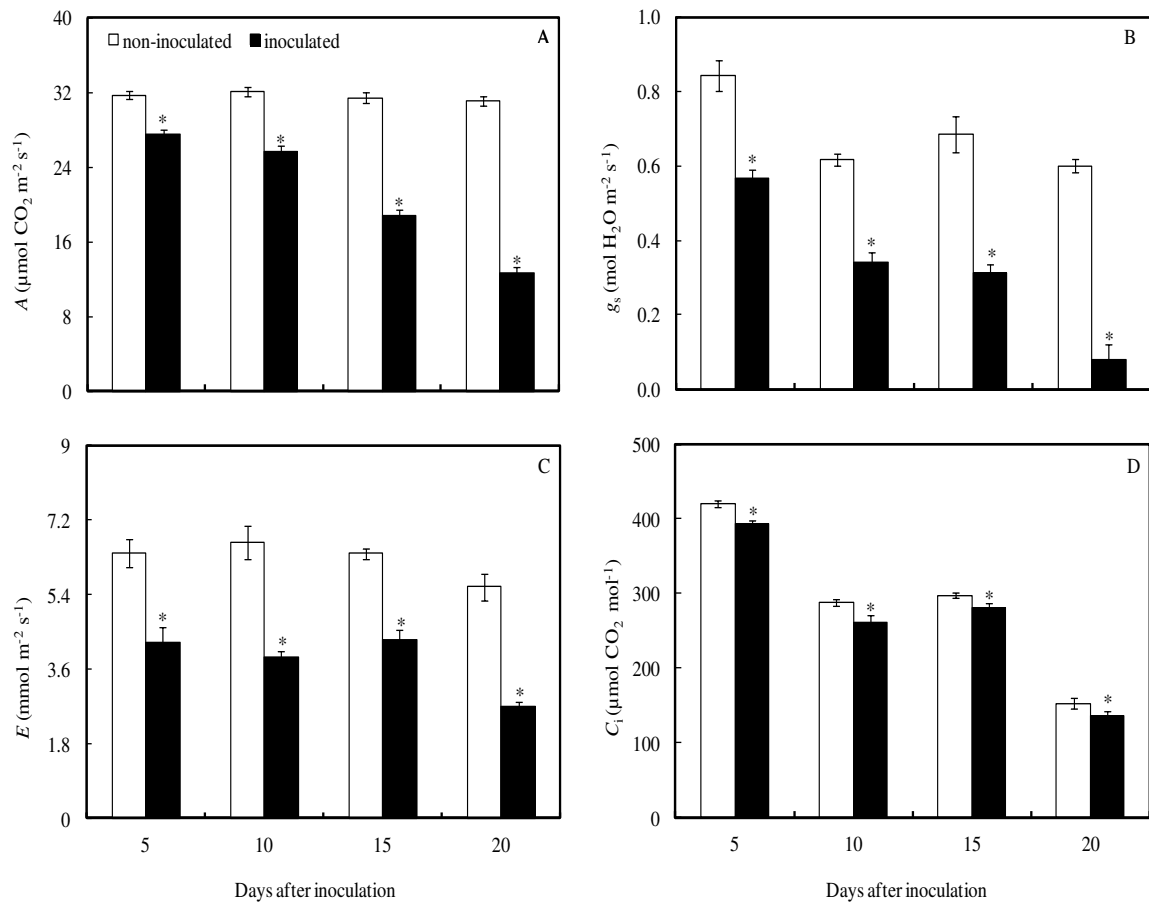


Figure 2

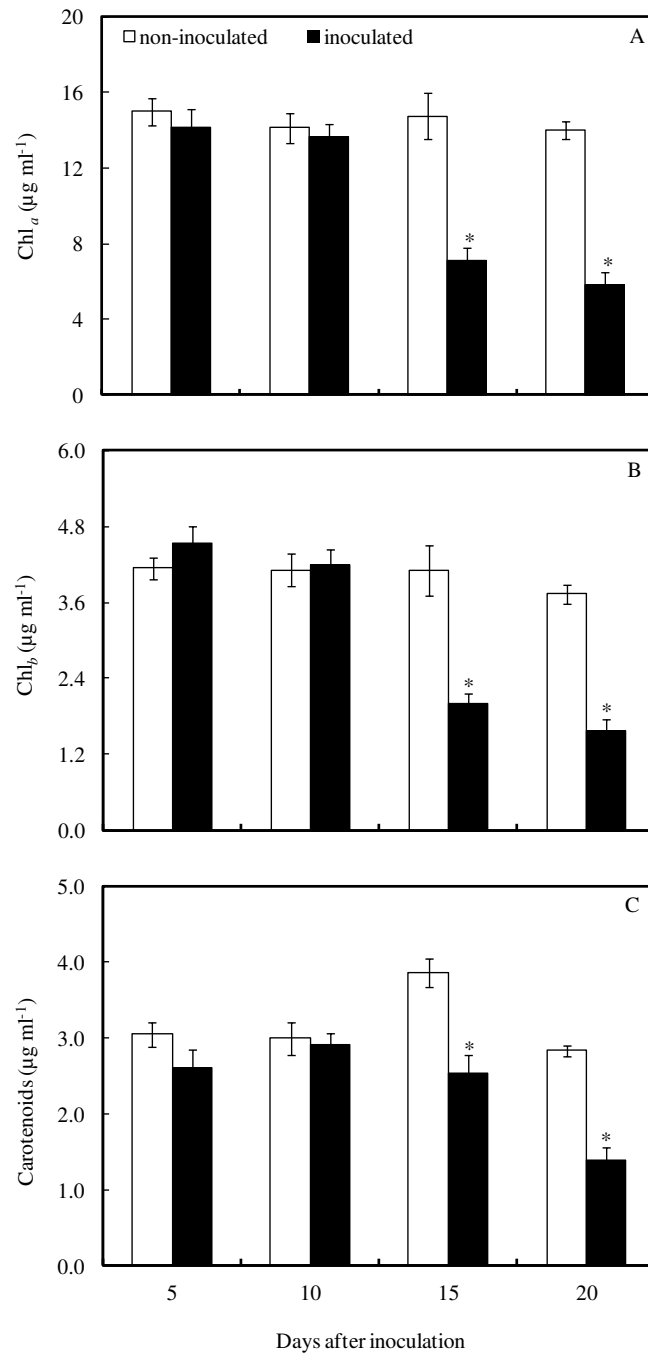


Figure 3

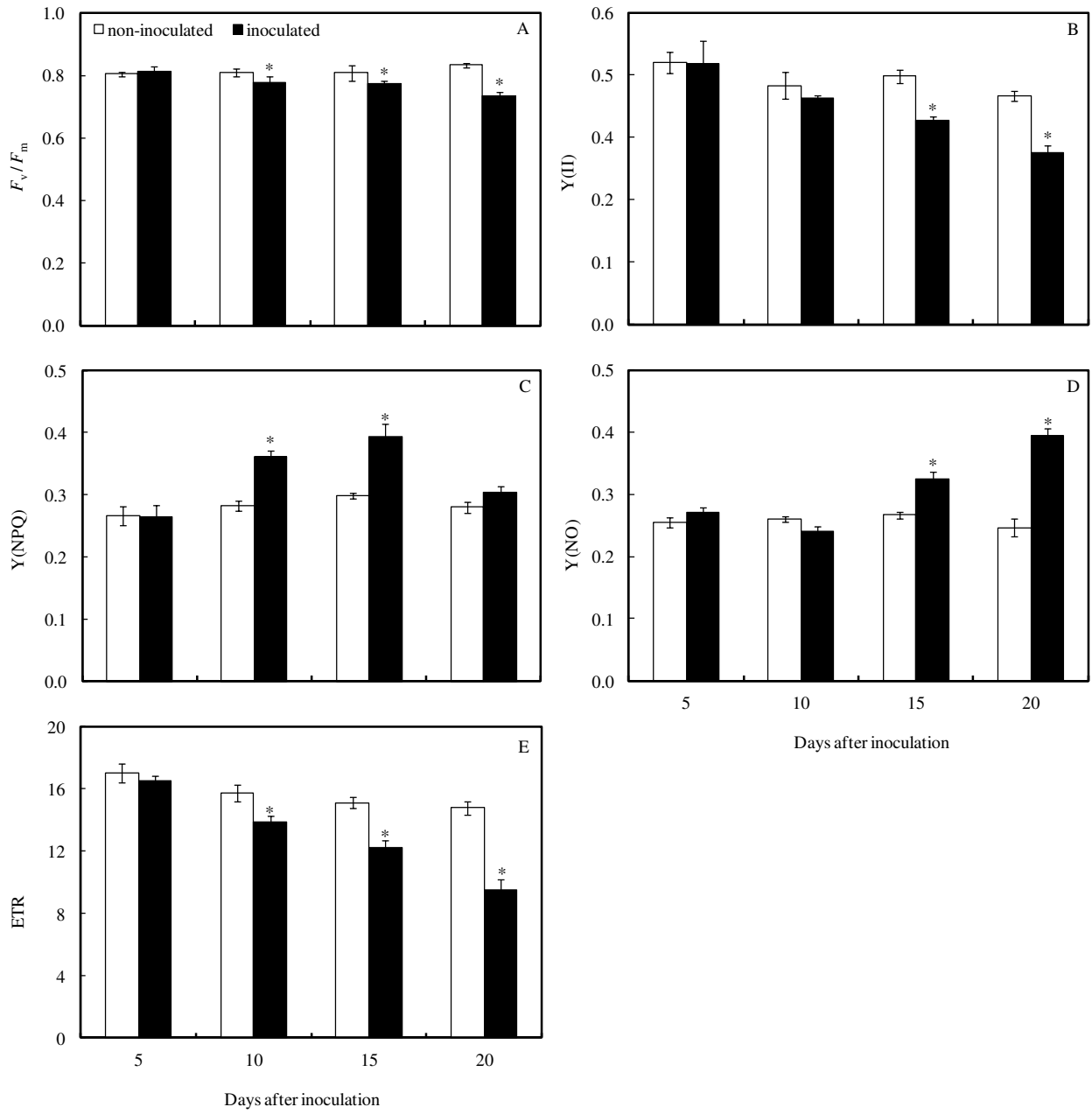


Figure 4

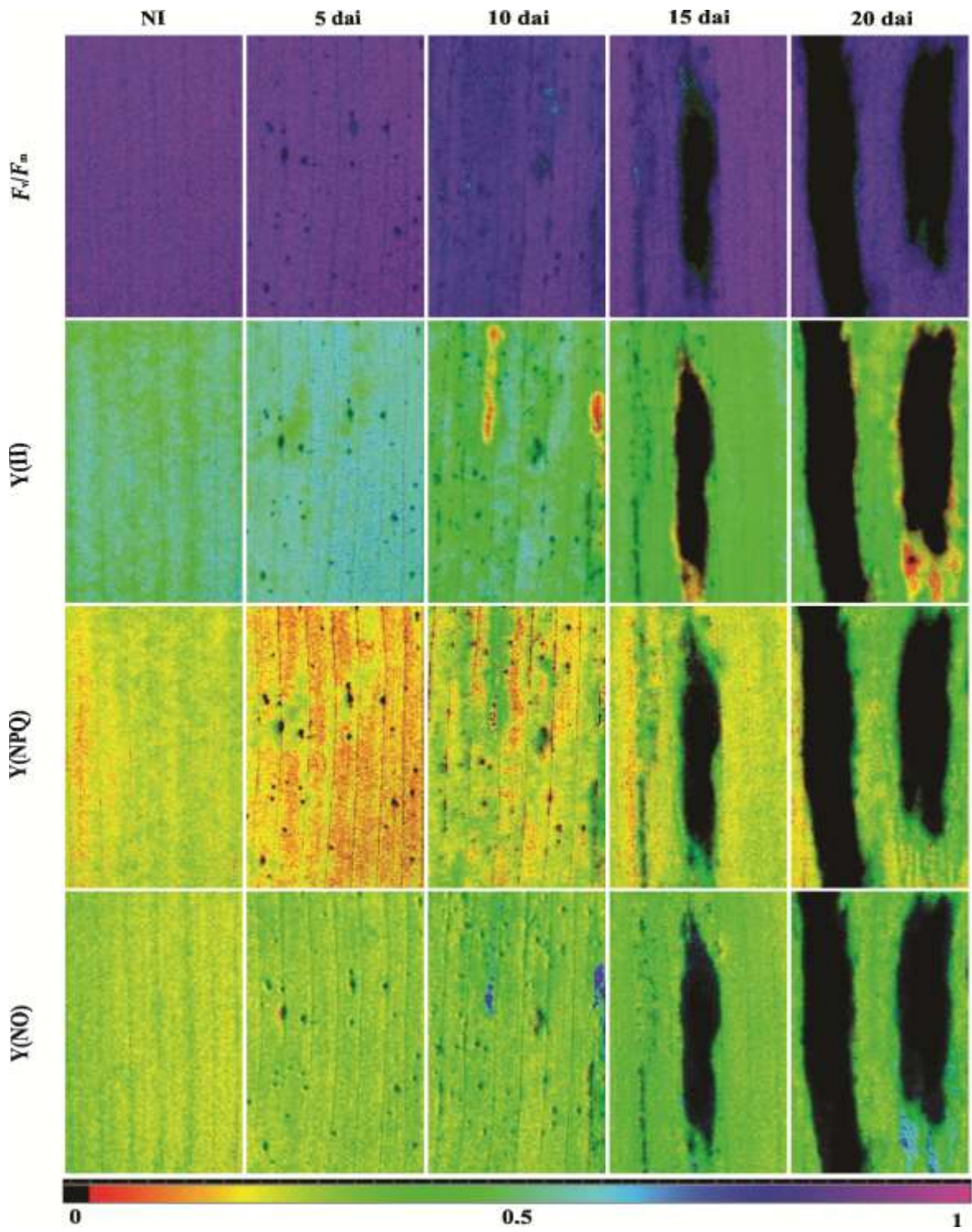


Figure 5